

# Weak lensing of gravitational waves in wave optics: Beyond the Born approximation

Morifumi Mizuno<sup>1</sup>, Teruaki Suyama<sup>1</sup>

<sup>1</sup>*Department of Physics, Tokyo Institute of Technology, 2-12-1 Ookayama, Meguro-ku, Tokyo 152-8551, Japan*

## Abstract

Universe’s matter inhomogeneity gravitationally affects the propagation of gravitational waves (GWs), causing the lensing effect. Particularly, the weak lensing of GWs contains abundance of information about the small scale matter power spectrum and it has been studied within the range of the Born approximation. In this work, we investigate the validity of the Born approximation by accounting for the higher order terms in the gravitational potential  $\Phi$ . We first develop the formulation of the post-Born approximation, which is made by introducing a new variable. We then derive the expression of the magnitude and the phase of the amplification factor up to third order in  $\Phi$  and compute the average and variance beyond the Born approximation. Our results suggest that the post-Born effect is indeed a few orders of magnitude smaller than the leading order contribution within almost all frequency ranges considered in this work except for the high frequency area  $f \sim 1000$  Hz, where the shot noise is dominant. Intriguingly, the number of necessary GW events for detecting the average, which originates purely from the post-Born effect, could become comparable or even smaller than the number required for detecting the variance, which appears at the level of the Born approximation. This indicates that the average is measurable with the same detection cost as the variance, even though it is only a few percent of the variance. On the other hand, we find that, even though the detection of the post-Born corrections to the variance would be possible in the case of the magnification, extracting the useful information to infer the shape of the matter power spectrum is still challenging even for the future generation GW detectors. This is due to the smallness of the post-Born effect and the difficulty of separating it from both the noise signal and the Born approximation effect.

## 1 Introduction

When light travels across the Universe, its trajectory is bent by the gravitational potential of intervening massive objects. This phenomena called gravitational lensing (GL) is quite

useful in astrophysics and cosmology (e.g., [1–3]). For instance, it can be used to measure the cosmological parameters. It can probe the abundance of dark compact objects.

According to general relativity, GL also occurs for the gravitational waves (GWs) [4]. One notable feature of the GL of GWs is that geometrical optics, which is a perfect approximation in most cases for light, no longer holds for GWs in some cases since the wavelength of GWs is typically much larger than that of light and diffraction effect becomes important [5–7]. In such cases, wave optics must be used to deal with the GL. In wave optics, contrary to the geometrical optics where the starting point is the lens equation, the lensing signal is represented by the so-called amplification factor defined as a ratio of the lensed waveform to the unlensed one (e.g., [8]). This quantity is a complex number and all the information of the lensing is encoded in it. Its absolute value and argument represent the amplification and phase modulation of the lensed wave, respectively.

In [9], GL of GWs caused by dark matter fluctuations was studied. It was shown that there is a length scale of the matter power spectrum below which the contribution to the lensing signal is suppressed due to wavy nature. This scale, *Fresnel scale*, depends on the GW frequency. Thus, by measuring the lensing signal at multiple frequencies and its frequency dependence, we can probe the matter power spectrum at the Fresnel scale. This idea has been investigated in more detail by updating the matter power spectrum as well as adding the compact objects in [10]. In [11], it was shown that the lensing signal of the dark matter fluctuations is hugely amplified by a massive object located on the line of sight which itself causes strong lensing.

When the lensing signal is weak, it is natural to keep only the terms first order in the gravitational potential  $\Phi$  (i.e. Born approximation). The contributions of the higher order terms are expected to be suppressed compared to the leading order contribution. In geometrical optics, this has been explicitly demonstrated in [12–16]. One naively expects that a similar conclusion can be drawn for the case of wave optics.

In [9], the amplification factor sourced by the dark matter fluctuations was obtained under the Born approximation (thus the variance of the lensing signal is second order in  $\Phi$ ). Typical magnitude of the amplitude and the phase fluctuations was found to be  $\mathcal{O}(10^{-2} - 10^{-3})$ . Thus, the lensing signal is weak and this would naturally justify the validity of the Born approximation. However, there are two issues that need to be investigated regarding the Born approximation. Firstly, although the post-Born corrections are expected to be small, it is not known how much they are suppressed actually. When the measurements of the lensing signal become available in the future, quantitative computation of the magnitude of the post-Born corrections is indispensable to correctly extract the matter power spectrum as well as to understand the level of the precision under consideration. Secondly, the Born approximation used in [9] apparently breaks down at large wave frequency since the gravitational potential in the wave equation is associated with the frequency. Notice that this issue does not appear in the geometrical optics since the lens equation is independent of the frequency of light. While it is known how the lens equation emerges in the wave optics, it is not obvious how the breakdown of the Born approximation for the large frequency in the wave optics is reconciled with the Born ap-

proximation in the geometric optics. In this paper, we take a first step towards addressing these issues by extending the previous studies to next higher orders in the gravitational potential. We first reformulate the wave equation to make its structure more tractable. We then derive the expression of the lensing signal up to third order in the gravitational potential. Expansion to this order is necessary to evaluate the variance of the post-Born corrections. As we will demonstrate, the post-Born corrections are suppressed by a few orders of magnitude compared to the leading order signal except in a high frequency region. Interestingly, when the post-Born corrections are included, the average of the lensing signal does not vanish. This average depends on the frequency in a non-trivial manner and thus cannot be absorbed into the change of the parameters characterizing the unlensed waveform. Our analysis suggests an interesting possibility to make use of the average of the lensing signal as an additional observable to probe the matter power spectrum.

## 2 Formulation

### 2.1 Lensing signal beyond the Born approximation

In this section, we reformulate the wave equation and show how the post-Born corrections are derived. Throughout this paper, we assume that the gravitational potential is small ( $\Phi \ll 1$ ) and the Universe is flat. We also ignore the polarization of GWs since the polarization tensor in the geometrical optics is parallel transported along the null geodesics [17] and hence the change of the polarization tensor would be suppressed by a factor of  $\mathcal{O}(\Phi)$  and observationally irrelevant.

The presence of mass fluctuation creates the distortion on spacetime, causing the deviation from the Friedmann–Lemaître–Robertson–Walker (FLRW) metric. This effect is small in most of the astrophysical situations and it is a good approximation to write the metric as [18]

$$ds^2 = g_{\mu\nu}^B dx^\mu dx^\nu = a^2(\eta)[- (1 + 2\Phi) d\eta^2 + (1 - 2\Phi) d\mathbf{x}^2], \quad (2.1)$$

where  $\eta$  and  $\mathbf{x}$  is a conformal time and a comoving coordinate, and  $a(\eta)$  is a scale factor. If the wavelength of GWs is much smaller than the typical radius of the curvature of the background metric, the propagation of GWs becomes the same as the wave equation of the massless scalar field  $\phi$ :  $\partial_\mu \left( \sqrt{-g^B} g_B^{\mu\nu} \partial_\nu \phi \right) = 0$ . The expansion of the Universe causes attenuation of  $\phi$  as  $\phi \propto 1/a$ . We extract this effect by redefining the GW amplitude  $\phi$  as  $\phi \rightarrow \phi/a$ . Then, the wave equation becomes [8]

$$(\nabla^2 + \omega^2) \tilde{\phi} = 4\omega^2 \Phi \tilde{\phi}, \quad (2.2)$$

in the frequency space.  $\tilde{\phi}(\omega, \mathbf{x})$  is the Fourier transform of  $\phi(\eta, \mathbf{x})$  <sup>#1</sup> and the higher order terms in  $\Phi$  have been ignored. It is common to represent the lensed waveform in terms of

---

<sup>#1</sup>It is defined by  $\phi(\eta, \mathbf{x}) = \int \frac{d\omega}{2\pi} e^{-i\omega\eta} \tilde{\phi}(\omega, \mathbf{x})$ . Thus,  $\omega$  is the comoving (angular) frequency.

the amplification factor, which is the ratio of the lensed and unlensed waveform, namely  $F = \tilde{\phi}/\tilde{\phi}_0$  [8], where the unlensed waveform is given by  $\tilde{\phi}_0 = e^{i\omega\chi}/\chi$  in terms of  $\chi$  which is the (comoving) distance from the source. Using the amplification factor  $F$ , Eq. (2.2) is rewritten as

$$2i\omega\frac{\partial F}{\partial\chi} + \frac{1}{\chi^2}\nabla_\theta^2 F = 4\omega^2\Phi F, \quad (2.3)$$

where the polar coordinate  $(\chi, \theta, \phi)$  is used and  $\nabla_\theta^2 = \partial^2/\partial\theta^2 + \sin\theta^{-1}\partial/\partial\theta + \sin\theta^{-2}\partial/\partial\phi^2$  is the 2 dimensional Laplace operator on 2-sphere. In Eq. (2.3), we have assumed GWs propagates along the line of sight and confined in the region  $\theta \ll 1$ . Therefore,  $\nabla_\theta$  can be interpreted as the operator on 2 dimensional flat surface perpendicular to the line of sight.

In order to evaluate the effects of the post-Born approximation, we find it convenient to deal with a new variable  $J$  defined as  $F = e^{i\omega J}$ . Using this new variable  $J$ , Eq. (2.3) becomes

$$\left(\frac{\partial}{\partial\chi} - \frac{i}{2\omega\chi^2}\nabla_\theta^2\right) J = -2\Phi - \frac{1}{2\chi^2}(\nabla_\theta J)^2. \quad (2.4)$$

This differential equation can be written as an integral equation by the Green function of the linear operator acting on the right-hand side,

$$J(\chi_s, \theta) = \int_0^{\chi_s} d\chi \exp\left[i\frac{W(\chi, \chi_s)\nabla_\theta^2}{2\omega}\right] \left(-2\Phi(\chi, \theta) - \frac{1}{2\chi^2}(\nabla_\theta J)^2\right), \quad (2.5)$$

where  $W(\chi, \chi_s) = \frac{1}{\chi} - \frac{1}{\chi_s}$ . In geometric optics,  $W(\chi, \chi_s)$  is sometimes called the lensing efficiency function [15]. The change of variable to  $J$  allows us to partially take into account the higher order terms in the gravitational potential which are not included in the previous studies [9, 10, 19]. Defining  $J^{(n)}$  as the term proportional to n-th order of the gravitational potential,  $J^{(n)}$  can be calculated iteratively order by order as

$$J^{(1)}(\chi_s, \theta) = \int_0^{\chi_s} d\chi \exp\left[i\frac{W(\chi, \chi_s)\nabla_\theta^2}{2\omega}\right] (-2\Phi(\chi, \theta)), \quad (2.6)$$

$$J^{(2)}(\chi_s, \theta) = - \int_0^{\chi_s} d\chi \exp\left[i\frac{W(\chi, \chi_s)\nabla_\theta^2}{2\omega}\right] \frac{(\nabla_\theta J^{(1)}(\chi, \theta))^2}{2\chi^2}, \quad (2.7)$$

$$J^{(3)}(\chi_s, \theta) = - \int_0^{\chi_s} d\chi \exp\left[i\frac{W(\chi, \chi_s)\nabla_\theta^2}{2\omega}\right] \frac{\nabla_\theta J^{(1)}(\chi, \theta) \cdot \nabla_\theta J^{(2)}(\chi, \theta)}{\chi^2}, \quad (2.8)$$

⋮

In the geometrical optics limit (i.e., large  $\omega$ ),  $\lim_{\omega \rightarrow \infty} J^{(n)}$  of any  $n$  becomes real and the correction term at  $\mathcal{O}(1/\omega)$  becomes imaginary. Thus,  $\lim_{\omega \rightarrow \infty} J$  is nothing but the difference between the arrival time of geodesic under the influence of  $\Phi$  and the one without  $\Phi$ . At the leading order, this reduces to the standard expression of the Shapiro time delay.

At  $\mathcal{O}(1/\omega)$ ,  $J$  gives the magnification in geometrical optics. In particular,  $i\omega J^{(1)}$  reduces to the standard formula of the convergence (e.g., [1, 2]).

In the literature, the Born approximation refers to the approximation to truncate the expansion of  $F$  up to first order in  $\Phi$ . Meanwhile, since our expansion is performed for  $J$ , even the truncation at  $J^{(1)}$  partially captures the higher order terms not included in the previous studies (see also the footnote #2). In spite of such a difference at the conceptual level, there is practically no difference as to whether the Born approximation refers to the first order truncation for  $F$  or  $J$  since the variation of  $F$  in the former case is nothing but  $J^{(1)}$ .

Our aim is to investigate the leading correction to the Born approximation of the lensing signal caused by the dark matter fluctuations. To this end, we compute the average and the variance of  $J$  and investigate how they are affected by the post-Born approximation by treating  $\Phi$  as a random variable. The average trivially vanishes in the Born approximation. Since the average of  $J^{(2)}$  does not vanish in general, we truncate the evaluation of the average at this order. The leading post-Born correction to the variance comes from the cross term  $J^{(1)}J^{(2)}$  and thus it is  $\mathcal{O}(\Phi^3)$ . This is non-vanishing only when  $\Phi$  is non-Gaussian. The next leading correction, which is  $\mathcal{O}(\Phi^4)$ , remains finite even when  $\Phi$  is Gaussian. Thus, the correction at  $\mathcal{O}(\Phi^4)$  may dominate over the one at  $\mathcal{O}(\Phi^3)$  in some cases, especially when  $\Phi$  is nearly Gaussian. Because of this reason, we compute the variance up to  $\mathcal{O}(\Phi^4)$ . To make our calculation consistent up to this order, we need to keep the expansion up to  $J^{(3)}$  since the cross term  $J^{(1)}J^{(3)}$  is  $\mathcal{O}(\Phi^4)$ .

For clarity, we define new differential operators  $(W\nabla)^{(2)}$  and  $(W\nabla)^{(3)}$  as

$$(W\nabla)^{(2)} = W(\chi, \chi_s) \nabla_{\theta_{12}}^2 + W(\chi_1, \chi) \nabla_{\theta_1}^2 + W(\chi_2, \chi) \nabla_{\theta_2}^2, \quad (2.9)$$

$$(W\nabla)^{(3)} = W(\chi, \chi_s) \nabla_{\theta_{123}}^2 + W(\chi_3, \chi) \nabla_{\theta_3}^2 + W(\chi', \chi) \nabla_{\theta_{12}}^2 \\ + W(\chi_1, \chi') \nabla_{\theta_1}^2 + W(\chi_2, \chi') \nabla_{\theta_2}^2. \quad (2.10)$$

Using these notations, we obtain the following expressions of  $J$  up to third order:

$$J^{(1)}(\chi_s, \theta) = -2 \int_0^{\chi_s} d\chi \exp \left[ i \frac{W(\chi, \chi_s) \nabla_{\theta}^2}{2\omega} \right] \Phi(\chi, \theta), \quad (2.11)$$

$$J^{(2)}(\chi_s, \theta) = -2 \int_0^{\chi_s} \frac{d\chi}{\chi^2} \int_0^{\chi} d\chi_1 \int_0^{\chi} d\chi_2 \exp \left[ i \frac{(W\nabla)^{(2)}}{2\omega} \right] \nabla_{\theta_1} \Phi_1 \cdot \nabla_{\theta_2} \Phi_2, \quad (2.12)$$

$$J^{(3)}(\chi_s, \theta) = -4 \int_0^{\chi_s} \frac{d\chi}{\chi^2} \int_0^{\chi} d\chi_3 \int_0^{\chi} \frac{d\chi'}{\chi'^2} \int_0^{\chi'} d\chi_1 \int_0^{\chi'} d\chi_2 \\ \times \exp \left[ i \frac{(W\nabla)^{(3)}}{2\omega} \right] \nabla_{\theta_{12}} (\nabla_{\theta_1} \Phi_1 \cdot \nabla_{\theta_2} \Phi_2) \cdot \nabla_{\theta_3} \Phi_3. \quad (2.13)$$

Note that  $\Phi_i = \Phi(\chi_i, \theta)$  and  $\nabla_{\theta_i}$  only acts on  $\Phi_i$  (when there are more than 2 subscript numbers at the corner of  $\nabla_{\theta}$ , it means the operator acts on the gravitational potentials that have the corresponding subscripts.).  $J^{(1)}$  corresponds to the Born approximation and subsequent terms ( $J^{(2)}$  and  $J^{(3)}$ ) are the post-Born corrections.

The information about the phase and the magnification of GWs is encoded in the real and imaginary part of  $J$ , respectively. Conventionally, the phase modulation and the magnification are denoted as  $S$  and  $K$  [9], and we follow the same notation in this paper.  $S$  and  $K$  are related to  $J$  as

$$S(\omega) = \omega \text{Re}(J), \quad (2.14)$$

$$K(\omega) = -\omega \text{Im}(J). \quad (2.15)$$

In this definition, the amplification factor is written as  $F(\omega) = e^{K(\omega)} e^{iS(\omega)}$  <sup>#2</sup>. As we have already pointed out, the Shapiro time delay describes the time lag caused by the gravitational potential. In the observation of GWs, the Shapiro time delay is not measurable. Therefore, this degree of freedom needs to be removed from the phase modulation. We redefine the physical phase modulation as

$$S_{\text{ph}}(\omega) = S(\omega) - \lim_{\omega \rightarrow \infty} S(\omega). \quad (2.16)$$

From now on, the term phase modulation always means this physical quantity even if it is not explicitly mentioned. With these in mind, the phase modulation and the magnification are then explicitly given by

$$S^{(1)} = -2\omega \int_0^{\chi_s} d\chi \left[ \cos \left[ \frac{W(\chi, \chi_s) \nabla_\theta^2}{2\omega} \right] - 1 \right] \Phi, \quad (2.17)$$

$$S^{(2)} = -2\omega \int_0^{\chi_s} \frac{d\chi}{\chi^2} \int_0^\chi d\chi_1 \int_0^\chi d\chi_2 \left[ \cos \left[ \frac{(W\nabla)^{(2)}}{2\omega} \right] - 1 \right] \nabla_{\theta_1} \Phi_1 \cdot \nabla_{\theta_2} \Phi_2, \quad (2.18)$$

$$S^{(3)} = -4\omega \int_0^{\chi_s} \frac{d\chi}{\chi^2} \int_0^\chi d\chi_3 \int_0^\chi \frac{d\chi'}{\chi'^2} \int_0^{\chi'} d\chi_1 \int_0^{\chi'} d\chi_2 \\ \times \left[ \cos \left[ \frac{(W\nabla)^{(3)}}{2\omega} \right] - 1 \right] \nabla_{\theta_{12}} (\nabla_{\theta_1} \Phi_1 \cdot \nabla_{\theta_2} \Phi_2) \cdot \nabla_{\theta_3} \Phi_3, \quad (2.19)$$

$$K^{(1)} = 2\omega \int_0^{\chi_s} d\chi \sin \left[ \frac{W(\chi, \chi_s) \nabla_\theta^2}{2\omega} \right] \Phi, \quad (2.20)$$

$$K^{(2)} = 2\omega \int_0^{\chi_s} \frac{d\chi}{\chi^2} \int_0^\chi d\chi_1 \int_0^\chi d\chi_2 \sin \left[ \frac{(W\nabla)^{(2)}}{2\omega} \right] \nabla_{\theta_1} \Phi_1 \cdot \nabla_{\theta_2} \Phi_2, \quad (2.21)$$

$$K^{(3)} = 4\omega \int_0^{\chi_s} \frac{d\chi}{\chi^2} \int_0^\chi d\chi_3 \int_0^\chi \frac{d\chi'}{\chi'^2} \int_0^{\chi'} d\chi_1 \int_0^{\chi'} d\chi_2 \\ \times \sin \left[ \frac{(W\nabla)^{(3)}}{2\omega} \right] \nabla_{\theta_{12}} (\nabla_{\theta_1} \Phi_1 \cdot \nabla_{\theta_2} \Phi_2) \cdot \nabla_{\theta_3} \Phi_3. \quad (2.22)$$

$S^{(1)}$  and  $K^{(1)}$  have been derived in the previous works [9, 10] and ours reproduce their results. To the best of our knowledge, higher order terms  $S^{(2)}$ ,  $S^{(3)}$ ,  $K^{(2)}$ ,  $K^{(3)}$  are the new

---

<sup>#2</sup>In [9, 10, 19],  $F$  was written as  $F = 1 + K + iS$ , then  $K$  and  $S$  were obtained up to first order in  $\Phi$ , and finally exponentiation  $F \approx (1 + K)e^{iS}$  was done. In our approach, the exponentiation procedure is naturally incorporated from the outset by using the variable  $J$ .

results. In the high frequency limit of Eqs. (2.20) and (2.21), the magnification computed from the above expressions reproduces the result derived in [12–16] under the post-Born approximation in geometric optics, which is demonstrated in appendix A.

## 2.2 Statistics of $K$ and $S$

The situation we have in mind is the lensing caused by the dark matter inhomogeneities randomly distributed in the whole Universe. This means that the  $K$  and  $S$  behave in a stochastic manner for individual GW events. Thus, the comparison between the theoretical prediction and observation is possible only for the statistical quantities. This motivates us to compute the average and the variance of the lensing signal.

To this end, we first notice that for the ensemble average of the functions of the gravitational potential, the following equations hold under the Limber approximation. For arbitrary functions  $F(x), G(x), H(x), I(x)$  of differential operator  $x$ , we have

$$\begin{aligned} & \langle F(\nabla_{\theta_1})\Phi_1 G(\nabla_{\theta_2})\Phi_2 \rangle \\ &= \delta^D(\chi_1 - \chi_2) \int \frac{d^2\mathbf{k}_\perp}{(2\pi)^2} F(i\chi_1\mathbf{k}_\perp) G(-i\chi_1\mathbf{k}_\perp) P_\Phi(k_\perp, \chi_1). \end{aligned} \quad (2.23)$$

$$\begin{aligned} & \langle F(\nabla_{\theta_1})\Phi_1 G(\nabla_{\theta_2})\Phi_2 H(\nabla_{\theta_3})\Phi_3 \rangle_c \\ &= \delta^D(\chi_1 - \chi_3)\delta^D(\chi_2 - \chi_3) \int \frac{d^2\mathbf{k}_{1\perp}}{(2\pi)^2} \int \frac{d^2\mathbf{k}_{2\perp}}{(2\pi)^2} \\ & \quad \times F(i\chi_3\mathbf{k}_{1\perp}) G(i\chi_3\mathbf{k}_{2\perp}) H(-i\chi_3\mathbf{k}_{1\perp} - i\chi_3\mathbf{k}_{2\perp}) B_\Phi(k_{1\perp}, k_{2\perp}, |\mathbf{k}_{1\perp} + \mathbf{k}_{2\perp}|, \chi_1) \end{aligned} \quad (2.24)$$

$$\begin{aligned} & \langle F(\nabla_{\theta_1})\Phi_1 G(\nabla_{\theta_2})\Phi_2 H(\nabla_{\theta_3})\Phi_3 I(\nabla_{\theta_4})\Phi_4 \rangle_c \\ &= \delta^D(\chi_1 - \chi_4)\delta^D(\chi_2 - \chi_4)\delta^D(\chi_3 - \chi_4) \int \frac{d^2\mathbf{k}_{1\perp}}{(2\pi)^2} \int \frac{d^2\mathbf{k}_{2\perp}}{(2\pi)^2} \int \frac{d^2\mathbf{k}_{3\perp}}{(2\pi)^2} \\ & \quad \times F(i\chi_4\mathbf{k}_{1\perp}) G(i\chi_4\mathbf{k}_{2\perp}) H(i\chi_4\mathbf{k}_{3\perp}) I(-i\chi_4\mathbf{k}_{1\perp} - i\chi_4\mathbf{k}_{2\perp} - i\chi_4\mathbf{k}_{3\perp}) \\ & \quad \times T_\Phi(\mathbf{k}_{1\perp}, \mathbf{k}_{2\perp}, \mathbf{k}_{3\perp}, -\mathbf{k}_{1\perp} - \mathbf{k}_{2\perp} - \mathbf{k}_{3\perp}, \chi_1). \end{aligned} \quad (2.25)$$

Here  $P_\Phi, B_\Phi, T_\Phi$  are the power spectrum, bispectrum, and trispectrum of  $\Phi$ , and  $\langle \dots \rangle_c$  indicates the connected term. They are characterized by

$$\langle \tilde{\Phi}(\mathbf{k}_1, \chi) \tilde{\Phi}(\mathbf{k}_2, \chi) \rangle = (2\pi)^3 \delta^D(\mathbf{k}_1 + \mathbf{k}_2) P_\Phi(k_1, \chi), \quad (2.26)$$

$$\langle \tilde{\Phi}(\mathbf{k}_1, \chi) \tilde{\Phi}(\mathbf{k}_2, \chi) \tilde{\Phi}(\mathbf{k}_3, \chi) \rangle_c = (2\pi)^3 \delta^D(\mathbf{k}_1 + \mathbf{k}_2 + \mathbf{k}_3) B_\Phi(k_1, k_2, k_3, \chi), \quad (2.27)$$

$$\langle \tilde{\Phi}(\mathbf{k}_1, \chi) \tilde{\Phi}(\mathbf{k}_2, \chi) \tilde{\Phi}(\mathbf{k}_3, \chi) \tilde{\Phi}(\mathbf{k}_4, \chi) \rangle_c = (2\pi)^3 \delta^D(\mathbf{k}_1 + \mathbf{k}_2 + \mathbf{k}_3 + \mathbf{k}_4) T_\Phi(\mathbf{k}_1, \mathbf{k}_2, \mathbf{k}_3, \mathbf{k}_4, \chi), \quad (2.28)$$

where  $\tilde{\Phi}(\mathbf{k})$  is the Fourier transform of  $\Phi$ . With these definitions, we are ready to derive



the average and the variance of the post-Born corrections, which we will address in the following.

### 2.2.1 Average

At the level of the Born approximation, the average of  $K$  and  $S$  is zero. This does not happen beyond the Born approximation. Thus, the average of  $K$  and  $S$  fully represents the effects of the post-Born corrections. The leading order correction is  $\mathcal{O}(\Phi^2)$ , and we evaluate  $\langle K \rangle, \langle S \rangle$  at this order. From Eqs (2.18), (2.21), and (2.23), we obtain the following expressions:

$$\langle S \rangle = 2\omega \int_0^{\chi_s} \frac{d\chi}{\chi^2} \int_0^\chi d\chi_1 \chi_1^2 \int \frac{d^2 k_\perp}{(2\pi)^2} k_\perp^2 \left( 1 - \cos \left[ \frac{(\chi - \chi_1)\chi_1}{\chi\omega} k_\perp^2 \right] \right) P_\Phi(k_\perp, \chi_1), \quad (2.29)$$

$$\langle K \rangle = -2\omega \int_0^{\chi_s} \frac{d\chi}{\chi^2} \int_0^\chi d\chi_1 \chi_1^2 \int \frac{d^2 k_\perp}{(2\pi)^2} k_\perp^2 \sin \left[ \frac{(\chi - \chi_1)\chi_1}{\chi\omega} k_\perp^2 \right] P_\Phi(k_\perp, \chi_1). \quad (2.30)$$

At this stage, there are three things worth mentioning. Firstly, it is suggestive to rewrite the above relations in terms of the filter functions  $F_S^{(2)}, F_K^{(2)}$  as

$$\langle S \rangle = 2 \int_0^{\chi_s} \frac{d\chi}{\chi^3} \int_0^\chi d\chi' \chi'^3 (\chi - \chi') \int \frac{dk}{2\pi} F_S^{(2)} k^5 P_\Phi(k, \chi'), \quad (2.31)$$

$$\langle K \rangle = -2 \int_0^{\chi_s} \frac{d\chi}{\chi^3} \int_0^\chi d\chi' \chi'^3 (\chi - \chi') \int \frac{dk}{2\pi} F_K^{(2)} k^5 P_\Phi(k, \chi'), \quad (2.32)$$

where

$$F_S^{(2)} = \frac{1 - \cos k^2 r_F^2}{k^2 r_F^2}, \quad F_K^{(2)} = \frac{\sin k^2 r_F^2}{k^2 r_F^2}, \quad (2.33)$$

and  $r_F$  defined by  $r_F^2 = \chi'(\chi - \chi')/(\omega\chi)$  is the Fresnel scale [9]. By writing in this way, it is manifest that the frequency dependence of  $\langle S \rangle$  and  $\langle K \rangle$  is solely encoded in the filter functions. These filter functions are suppressed below the Fresnel scale  $k^{-1} < r_F$ . Physically, the filter functions describe the diffraction effect that lowers the lensing signal when the size of matter fluctuations is below this scale. In [9], it was argued that  $\langle S^2 \rangle$  and  $\langle K^2 \rangle$  (within the Born approximation) are insensitive to the matter fluctuations below the Fresnel scale. Our result demonstrates that the similar conclusion holds for  $\langle S \rangle, \langle K \rangle$ . Secondly, since, unlike in the case of geometric optics, both  $\langle S \rangle$  and  $\langle K \rangle$  depend on the GW frequency due to the frequency dependence of the Fresnel scale, we can extract the matter power spectrum at the Fresnel scale by measuring  $\langle S \rangle$  and  $\langle K \rangle$  at multiple frequencies and how they vary as the frequency is changed. This suggests a possibility that, in addition to  $\langle S^2 \rangle$  and  $\langle K^2 \rangle$ ,  $\langle S \rangle$  and  $\langle K \rangle$  can be used as a new observables to probe the matter power spectrum at the Fresnel scale. Notice that, contrary to the case of the cosmological perturbations where the average of the perturbations is absorbed into the FLRW background,  $\langle S \rangle$  and  $\langle K \rangle$  cannot be absorbed into the unlensed waveform since i) the frequency dependence of the average is different from that of the unlensed waveform



and ii) each merger event has different unlensed waveform. Thirdly,  $\langle S \rangle$  is positive definite for any  $\omega$ . Thus, if the measurement of  $\langle S \rangle$  gives a negative value, we can robustly conclude that it is not due to the lensing by the matter fluctuations but due to something else.

### 2.2.2 Variance

In the same way, the rms of the magnification up to forth order in  $\Phi$  is given by

$$\langle K^2 \rangle = \langle (K^{(1)})^2 \rangle + 2 \langle K^{(1)} K^{(2)} \rangle + 2 \langle K^{(1)} K^{(3)} \rangle + \langle (K^{(2)})^2 \rangle. \quad (2.34)$$

The variance of the magnification up to the same order is then written as  $\Delta_K^2 = \langle K^2 \rangle - \langle K^{(2)} \rangle^2$ . We define the post-Born corrections to the variance as  $\Delta_K^2 = \langle K_{\text{Born}}^2 \rangle + \delta_{K^2}$ . In this definition, it is possible that  $\delta_{K^2} < 0$ . As we mentioned earlier, the third order term in  $\Phi$  is necessary because it couples with the first order term. At this order, the result will depend on whether  $\Phi$  is Gaussian or non-Gaussian. In the diagrammatic language, the variance contains both disconnected ( $\delta_{K^2, \text{dc}}$ ) and connected ( $\delta_{K^2, \text{c}}$ ) parts:

$$\delta_{K^2} = \delta_{K^2, \text{dc}} + \delta_{K^2, \text{c}} \quad (2.35)$$

As for the disconnected part, we find that it consists of the three distinct terms:

$$\delta_{K^2, \text{dc}} = \langle (K^{(2)})^2 \rangle_{\text{dc}} + 2 \langle K^{(1)} K^{(3)} \rangle_{\text{dc}} - \langle K^{(2)} \rangle_{\text{dc}}^2, \quad (2.36)$$

where the subscript dc should be understood that the corresponding quantity is obtained by treating  $\Phi$  as a Gaussian variable. The connected part also consists of three terms:

$$\delta_{K^2, \text{c}} = 2 \langle K^{(1)} K^{(2)} \rangle_{\text{c}} + 2 \langle K^{(1)} K^{(3)} \rangle_{\text{c}} + \langle (K^{(2)})^2 \rangle_{\text{c}}. \quad (2.37)$$

The first term in Eq. (2.34) is nothing but the variance in the Born approximation and has been already derived in the literature [9]. For completeness, we will provide its expression below. For the Gaussian variable, n-point correlation function is completely specified by the two-point function, i.e., the matter power spectrum. Using this fact, we

find that each term can be written as

$$\langle (K^{(1)})^2 \rangle = 4\omega^2 \int_0^{\chi_s} d\chi \int \frac{d^2 k_\perp}{(2\pi)^2} \sin^2 \left[ \frac{(\chi_s - \chi)\chi}{2\chi_s\omega} k_\perp^2 \right] P_\Phi(k_\perp), \quad (2.38)$$

$$\begin{aligned} \langle (K^{(2)})^2 \rangle_{\text{dc}} &= \langle K^{(2)} \rangle_{\text{dc}}^2 + 16\omega^2 \int_0^{\chi_s} \frac{d\chi}{\chi^2} \int_0^\chi \frac{d\chi'}{\chi'^2} \int_0^{\chi'} d\chi_1 \int_0^{\chi'} d\chi_2 \int \frac{d^2 k_{1\perp}}{(2\pi)^2} \int \frac{d^2 k_{2\perp}}{(2\pi)^2} \\ &\quad \times \sin \left[ \frac{(\chi_s - \chi_1)\chi_1}{2\chi_s\omega} k_{1\perp}^2 + \frac{(\chi_s - \chi_2)\chi_2}{2\chi_s\omega} k_{2\perp}^2 + \frac{(\chi_s - \chi)\chi_1\chi_2}{\omega\chi_s\chi} \mathbf{k}_{1\perp} \cdot \mathbf{k}_{2\perp} \right] \\ &\quad \times \sin \left[ \frac{(\chi_s - \chi_1)\chi_1}{2\chi_s\omega} k_{1\perp}^2 + \frac{(\chi_s - \chi_2)\chi_2}{2\chi_s\omega} k_{2\perp}^2 + \frac{(\chi_s - \chi')\chi_1\chi_2}{\omega\chi_s\chi'} \mathbf{k}_{1\perp} \cdot \mathbf{k}_{2\perp} \right] \\ &\quad \times \chi_1^2 \chi_2^2 (\mathbf{k}_{1\perp} \cdot \mathbf{k}_{2\perp})^2 P_\Phi(k_{1\perp}) P_\Phi(k_{2\perp}), \end{aligned} \quad (2.39)$$

$$\begin{aligned} \langle K^{(1)} K^{(3)} \rangle_{\text{dc}} &= -16\omega^2 \int_0^{\chi_s} \frac{d\chi}{\chi^2} \int_0^\chi \frac{d\chi'}{\chi'^2} \int_0^{\chi'} d\chi_1 \int_0^{\chi'} d\chi_2 \int \frac{d^2 k_{1\perp}}{(2\pi)^2} \int \frac{d^2 k_{2\perp}}{(2\pi)^2} \\ &\quad \times \sin \left[ \frac{(\chi_s - \chi_2)\chi_2}{2\chi_s\omega} k_{2\perp}^2 \right] \sin \left[ \frac{(\chi_s - \chi_2)\chi_2}{2\chi_s\omega} k_{2\perp}^2 + \frac{(\chi - \chi')\chi_1\chi_2}{\omega\chi\chi'} \mathbf{k}_{1\perp} \cdot \mathbf{k}_{2\perp} + \frac{(\chi - \chi_1)\chi_1}{\chi\omega} k_{1\perp}^2 \right] \\ &\quad \times (\chi_1^2 \chi_2^2 (\mathbf{k}_{1\perp} \cdot \mathbf{k}_{2\perp})^2 + \chi_1^3 \chi_2 k_{1\perp}^2 (\mathbf{k}_{1\perp} \cdot \mathbf{k}_{2\perp})) P_\Phi(k_{1\perp}) P_\Phi(k_{2\perp}). \end{aligned} \quad (2.40)$$

As these expressions show, the computations of  $\delta_{K^2, \text{dc}}$  requires multiple integration in eight variables. Among the eight variables, the integral with respect to the angle between  $\mathbf{k}_{1\perp}$  and  $\mathbf{k}_{2\perp}$  can be analytically performed and the result is written in terms of the Bessel functions. Thus, practically, the number of variables in the integration is seven. The concrete expression of  $\delta_{K^2, \text{dc}}$  which we will evaluate numerically in the next section is given in Appendix B.

The connected part  $\delta_{K^2, c}$  given by Eq. (2.37) comes from the non-Gaussianity of the matter fluctuations: the matter bispectrum and trispectrum, and so forth. The first term in Eq. (2.37), which is  $\mathcal{O}(\Phi^3)$ , is written in terms of the bispectrum as

$$\begin{aligned} \langle K^{(1)} K^{(2)} \rangle_c &= -4\omega^2 \int_0^{\chi_s} \frac{d\chi}{\chi^2} \int_0^\chi d\chi_3 \chi_3^2 \int \frac{d^2 k_{1\perp}}{(2\pi)^2} \int \frac{d^2 k_{2\perp}}{(2\pi)^2} \\ &\quad \times \sin \left[ \frac{(\chi_s - \chi_3)\chi_3}{2\omega\chi_s} |\mathbf{k}_{1\perp} + \mathbf{k}_{2\perp}|^2 \right] \sin \left[ \frac{(\chi_s - \chi_3)\chi_3}{2\omega\chi_s} (k_{1\perp}^2 + k_{2\perp}^2) + \frac{(\chi_s - \chi)\chi_3^2}{\omega\chi_s\chi} \mathbf{k}_{1\perp} \cdot \mathbf{k}_{2\perp} \right] \\ &\quad \times (\mathbf{k}_{1\perp} \cdot \mathbf{k}_{2\perp}) B_\Phi(k_{1\perp}, k_{2\perp}, |\mathbf{k}_{1\perp} + \mathbf{k}_{2\perp}|). \end{aligned} \quad (2.41)$$

The other two terms, which are  $\mathcal{O}(\Phi^4)$ , are written in terms of the trispectrum as

$$\begin{aligned}
\langle (K^{(2)})^2 \rangle_c &= -8\omega^2 \int_0^{\chi_s} \frac{d\chi}{\chi^2} \int_0^\chi \frac{d\chi'}{\chi'^2} \int_0^{\chi'} d\chi_4 \chi_4^4 \int \frac{d^2 k_{1\perp}}{(2\pi)^2} \int \frac{d^2 k_{2\perp}}{(2\pi)^2} \int \frac{d^2 k_{3\perp}}{(2\pi)^2} \\
&\times \sin \left[ \frac{(\chi_s - \chi)\chi_4^2}{2\omega\chi_s\chi} |\mathbf{k}_{1\perp} + \mathbf{k}_{2\perp}|^2 + \frac{(\chi - \chi_4)\chi_4}{2\omega\chi} (k_{1\perp}^2 + k_{2\perp}^2) \right] \\
&\times \sin \left[ \frac{(\chi_s - \chi')\chi_4^2}{2\omega\chi_s\chi'} |\mathbf{k}_{1\perp} + \mathbf{k}_{2\perp}|^2 + \frac{(\chi' - \chi_4)\chi_4}{2\omega\chi'} (k_{3\perp}^2 + |\mathbf{k}_{1\perp} + \mathbf{k}_{2\perp} + \mathbf{k}_{3\perp}|^2) \right] \\
&\times (\mathbf{k}_{1\perp} \cdot \mathbf{k}_{2\perp}) [\mathbf{k}_{3\perp} \cdot (\mathbf{k}_{1\perp} + \mathbf{k}_{2\perp} + \mathbf{k}_{3\perp})] T_\Phi(\mathbf{k}_{1\perp}, \mathbf{k}_{2\perp}, \mathbf{k}_{3\perp}, -\mathbf{k}_{1\perp} - \mathbf{k}_{2\perp} - \mathbf{k}_{3\perp}). \tag{2.42}
\end{aligned}$$

$$\begin{aligned}
\langle K^{(1)} K^{(3)} \rangle_c &= 8\omega^2 \int_0^{\chi_s} \frac{d\chi}{\chi^2} \int_0^\chi \frac{d\chi'}{\chi'^2} \int_0^{\chi'} d\chi_4 \chi_4^4 \int \frac{d^2 k_{1\perp}}{(2\pi)^2} \int \frac{d^2 k_{2\perp}}{(2\pi)^2} \int \frac{d^2 k_{3\perp}}{(2\pi)^2} \\
&\times \sin \left[ \frac{(\chi_s - \chi_4)\chi_4}{2\omega\chi_s} |\mathbf{k}_{1\perp} + \mathbf{k}_{2\perp} + \mathbf{k}_{3\perp}|^2 \right] \\
&\times \sin \left[ \frac{(\chi_s - \chi)\chi_4^2}{2\omega\chi_s\chi} |\mathbf{k}_{1\perp} + \mathbf{k}_{2\perp} + \mathbf{k}_{3\perp}|^2 + \frac{(\chi - \chi_4)\chi_4}{2\omega\chi} k_{3\perp}^3 \right. \\
&\quad \left. + \frac{(\chi - \chi')\chi_4^2}{2\omega\chi\chi'} |\mathbf{k}_{1\perp} + \mathbf{k}_{2\perp}|^2 + \frac{(\chi' - \chi_4)\chi_4}{2\omega\chi'} (k_{1\perp}^2 + k_{2\perp}^2) \right] \\
&\times (\mathbf{k}_{1\perp} \cdot \mathbf{k}_{2\perp}) [(\mathbf{k}_{1\perp} + \mathbf{k}_{2\perp}) \cdot \mathbf{k}_{3\perp}] T_\Phi(\mathbf{k}_{1\perp}, \mathbf{k}_{2\perp}, \mathbf{k}_{3\perp}, -\mathbf{k}_{1\perp} - \mathbf{k}_{2\perp} - \mathbf{k}_{3\perp}). \tag{2.43}
\end{aligned}$$

In order to evaluate the connected part, we need to determine the bispectrum and the trispectrum of the matter fluctuations, which is beyond the scope of this paper. In what follows, we only focus on the disconnected part.

The above formulation is for the variance of  $K$ . The variance of  $S$  can be formulated in exactly the same manner. The quantities of  $S$  corresponding to Eqs. (2.38), (2.39), (2.40), (2.41), (2.42), and (2.43) are obtained by replacing all the sine functions as  $\sin(\dots) \rightarrow 1 - \cos(\dots)$ .

### 3 Post-Born effect on $S$ and $K$

Our results in the previous section are described by the power spectrum of the potential  $P_\Phi(k, \chi)$ . In the actual computations of the average and the variance of  $S$  and  $K$ , this is obtained from the matter power spectrum through the Poisson equation:

$$P_\Phi(k, \chi) = \left( \frac{3H_0^2 \Omega_m}{2} \right)^2 \frac{1}{a^2(\chi) k^4} P_\delta(k, \chi). \tag{3.1}$$

The precise dependence of the matter power spectrum at small scale, which is important for the frequency range of our interest, is very difficult to compute from the first principle. Alternatively, the halo model provides a useful phenomenological approach to obtain the

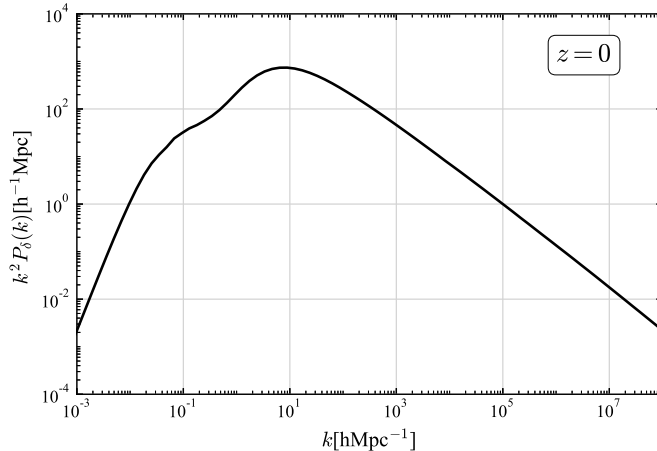


**Figure 1:** The matter power spectrum at  $z = 0$  obtained via the halo model at  $z = 0$  without including the shot noise coming from the Poisson distributed stars which dominate at small scales. At large  $k$ ,  $P_\delta$  obeys a single power-law ( $P_\delta \propto k^{-b}$ ). In numerical calculation, we set the range of  $k$  integral from  $10^{-4} h\text{Mpc}^{-1}$  to  $10^{12} h\text{Mpc}^{-1}$ . We do not show the entire integral range in this figure because the lower and higher end of  $P_\delta$  do not contribute to  $K$  and  $S$  as much as the area shown here does.

matter power spectrum. In this section, we adopt the formulation of the halo model described in [10] and compute  $P_\delta$  numerically. For technical reason, we do not include matter fluctuations coming from the Poisson distribution of stars (and possibly other type of compact objects) which contribute as a shot noise to the matter power spectrum and dominate at small scales. The contribution from the shot noise is separately studied in 3.4.

Fig. 1 shows the matter power spectrum used in our calculation at  $z = 0$ . We use this power spectrum and perform the numerical calculation of the average and the variance of  $S$  and  $K$ . We then compare the results with those obtained under the Born approximation. We set the range of  $k$  integral from  $10^{-4} h\text{Mpc}^{-1}$  to  $10^{12} h\text{Mpc}^{-1}$ . The cosmological parameters we use in this paper are  $h = 0.7, \Omega_m = 0.3, \Omega_\Lambda = 0.7$ .

Finally, we note that at large  $k$ ,  $P_\delta$  is given by a single power-law as

$$P_\delta(k, \chi) = B(\chi)k^{-b}, \quad (3.2)$$

where  $b = 2.87$  at  $z = 0$ . This form is useful to approximately evaluate the asymptotic behavior of the average and the variance of  $S$  and  $K$ , which we will address later.

### 3.1 Born approximation

For completeness, we first evaluate the variance of  $S$  and  $K$  under the Born approximation. Formally,  $\langle K_{\text{Born}}^2 \rangle$  is given by Eq. (2.38) and  $\langle S_{\text{Born}}^2 \rangle$  is given by the same equation with

sin function being replaced with  $1 - \cos$ . The purple curve in Fig. 2a shows  $\langle S_{\text{Born}}^2 \rangle^{1/2}$  as a function of GW frequency  $f$  when the source redshift is  $z_s = 3$ . It has a peak at frequency around  $10^{-11}$  Hz, which reflects the peak in the matter power spectrum seen in Fig. 1. Below(above) this frequency,  $\langle S_{\text{Born}}^2 \rangle$  increases(decreases) as the frequency is increased. In order to understand this feature, let us write  $\langle S_{\text{Born}}^2 \rangle$  in terms of the matter power spectrum as

$$\langle S_{\text{Born}}^2 \rangle = 4\omega^2 \left( \frac{3H_0^2 \Omega_m}{2} \right)^2 \int_0^{\chi_s} \frac{d\chi}{a^2(\chi)} \int \frac{dk}{2\pi k^3} \left( 1 - \cos \left[ \frac{(\chi_s - \chi)\chi}{2\chi_s \omega} k^2 \right] \right)^2 P_\delta(k, \chi). \quad (3.3)$$

The integration over  $k$  is dominated by the integrand around the scale where the argument of the cosine function becomes  $\mathcal{O}(1)$ . Thus, approximating  $P_\delta$  at that scale as a single-power law  $P_\delta \propto k^n$  ( $n \sim 1$  at the low frequency side and  $n = -b$  at the high frequency side), we find the scaling  $\langle S_{\text{Born}}^2 \rangle \propto \omega^{1+\frac{n}{2}}$ , which explains the asymptotic behavior of the purple curve. Notice that the Taylor-expansion of the cosine in the powers of  $1/\omega$  in the high frequency regime, which naively gives the scaling  $\langle S_{\text{Born}}^2 \rangle \propto \omega^{-2}$ , does not make sense due to the divergence of  $k$  integration stemming from the coefficient of  $\omega^{-2}$ . The fact that the scaling of  $\langle S_{\text{Born}}^2 \rangle$  at higher frequency range depends on  $b$  suggests an interesting possibility that the measurement of the frequency dependence of  $\langle S_{\text{Born}}^2 \rangle$  provides a direct probe of the slope of the matter spectrum at small scales.

The orange curve in Fig. 2b shows  $\langle K_{\text{Born}}^2 \rangle^{1/2}$  as a function of  $f$ . Contrary to the phase modulation, the variance of  $K$  approaches a constant value in the high frequency limit, which is nothing but the variance of the convergence in geometrical optics. In the frequency range lower than  $10^{-11}$  Hz,  $\langle K_{\text{Born}}^2 \rangle$  decreases as the frequency is lowered. In order to understand this feature, let us write  $\langle K_{\text{Born}}^2 \rangle$  in terms of the matter power spectrum as

$$\langle K_{\text{Born}}^2 \rangle = 4\omega^2 \left( \frac{3H_0^2 \Omega_m}{2} \right)^2 \int_0^{\chi_s} \frac{d\chi}{a^2(\chi)} \int \frac{dk}{2\pi k^3} \sin^2 \left[ \frac{(\chi_s - \chi)\chi}{2\chi_s \omega} k^2 \right] P_\delta(k, \chi). \quad (3.4)$$

Below the critical frequency  $10^{-11}$  Hz, the same argument as in the case for the phase modulation gives the scaling  $\langle K_{\text{Born}}^2 \rangle \propto \omega^{1+\frac{n}{2}}$  for small  $\omega$ .

## 3.2 Average

Having understood the behaviors of the amplitude and phase modulations in the Born approximation, let us proceed to the post-Born corrections. The dashed cyan curve in Fig. 2a shows  $\langle S \rangle$  as a function of GW frequency  $f$  numerically computed based on Eq. (2.31) with all sin functions being replaced with  $1 - \cos$  combined with Eq. (3.1). The source redshift is taken to be  $z_s = 3$ . As mentioned in the previous section,  $\langle S \rangle$  is always positive and our numerical result indeed indicates so. We find that the magnitude of  $\langle S \rangle$  reaches maximum at  $f = 3 \times 10^{-11}$  Hz and is 4% of  $\langle S_{\text{Born}}^2 \rangle^{1/2}$ . Then,  $|\langle S \rangle| / \langle S_{\text{Born}}^2 \rangle^{1/2}$  decreases as the frequency of GWs becomes larger. It is also important to observe that  $\langle S \rangle$  is more

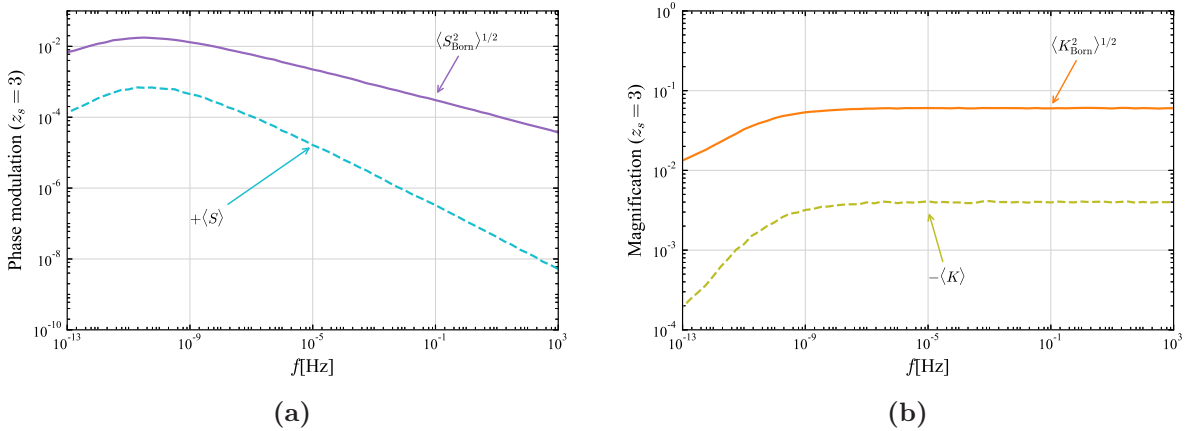


**Figure 2:** (a) The purple solid curve and the dashed cyan curve show  $\langle S_{\text{Born}}^2 \rangle^{1/2}$  and  $\langle S \rangle$ , respectively. The ratio of the latter to the former is maximum (4%) at  $f = 3 \times 10^{-11}$  Hz, and it decreases as  $f$  becomes larger. Within this high frequency range, we see that the numerical results coincide with the asymptotic behavior ( $\langle S_{\text{Born}}^2 \rangle^{1/2} \propto f^{-(b-2)/4}$  and  $\langle S \rangle \propto f^{-(b-2)/2}$ ,  $b \sim 2.87$ ) which is derived by analytic calculations. (b) The orange solid curve and olive dashed curve show  $\langle K_{\text{Born}}^2 \rangle^{1/2}$  and  $\langle K \rangle$ , respectively. Our calculation shows that  $\langle K \rangle$  is always negative within our frequency range. In the detectable frequency range,  $\langle K \rangle$  is 6% of  $\langle K_{\text{Born}}^2 \rangle^{1/2}$ . In both calculations, the source redshift is taken to be  $z_s = 3$ .

strongly suppressed than  $\langle S_{\text{Born}}^2 \rangle^{1/2}$  in a high frequency region. This can be explained by the asymptotic behavior of  $S$ , which is described by  $\langle S_{\text{Born}}^2 \rangle^{1/2} \propto \omega^{-(b-2)/4}$  (see previous subsection) and  $\langle S \rangle \propto \omega^{-(b-2)/2}$  whose scaling can be obtained by the same argument as the one used for  $\langle S_{\text{Born}}^2 \rangle^{1/2}$ .

The olive dashed curve in Fig. 2b shows  $\langle K \rangle$ . We find that  $\langle K \rangle$  is always negative within the frequency range of our calculation, which is not obvious from the formulation of  $\langle K \rangle$ . As for the magnitude of  $\langle K_{\text{Born}}^2 \rangle^{1/2}$  and  $|\langle K \rangle|$ , they both reach the maximum value at around  $f \sim 10^{-7}$  [Hz] and stay the same at larger frequency. At current detectable frequency (10~1000 Hz),  $|\langle K \rangle|$  is 6% of  $\langle K_{\text{Born}}^2 \rangle^{1/2}$ , suggesting that the constant demagnification of  $K$  is happening. On the other hand, it is clear that  $\langle K \rangle$  is suppressed rapidly at low frequencies. This is consistent with our knowledge that the Born approximation should be well justified at small  $\omega$ .

### 3.3 Variance

Fig. 3a and Fig. 3b show the post-Born correction  $\delta_{S^2, \text{dc}}$  to the variance of the phase modulation  $S$  when the source redshift is  $z_s = 1$  and  $z_s = 3$ , respectively. The square of the average  $\langle S \rangle^2$  is also shown as a reference. Overall, the post-Born correction is suppressed

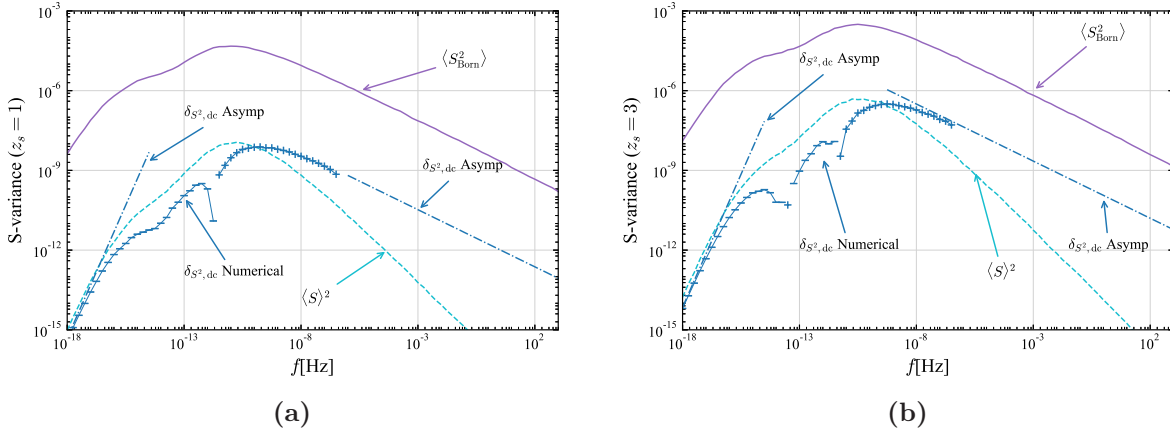


**Figure 3:** The source redshift of (a) is  $z_s = 1$  and (b) is  $z_s = 3$ . In both figures, the purple curve shows  $\langle S_{\text{Born}}^2 \rangle$ .  $\langle S \rangle^2$  is also shown as the cyan dashed curve for comparison.  $\delta_{S^2,dc}$  is plotted with blue markers and lines. At small frequency ( $f < 10^{-7}$  [Hz]), the result of the full numerical integral is plotted with markers(+, -). The shape of the markers indicates the signature of  $\delta_{S^2,dc}$  ( +, -  $\longleftrightarrow$   $\delta_{S^2,dc} > 0, < 0$ ). The straight lines at the lower end of both figures are the low frequency limit of  $\delta_{S^2,dc}$  given by Eq. (3.5). When the frequency is very low,  $\delta_{S^2,dc}$  is negative but  $\delta_{S^2,dc}$  becomes positive as  $\omega$  increases. We have not determined at which frequency this turnover occurs. The blue straight line at large  $k$  is the asymptotic behavior of  $\delta_{S^2,dc}$  calculated by (3.6).

compared to the leading term given by the Born approximation. Quantitatively, the degree of suppression depends on the frequency, as we will discuss below.

First, in the low frequency side,  $\delta_{S^2,dc}$  is more suppressed than  $\langle S_{\text{Born}}^2 \rangle$ . To understand this result, let us look at the expression of  $\delta_{S^2,dc}$  which is given in the Appendix B. When the frequency is sufficiently small, the products of the function  $F(x) = 1 - \cos x$ , which is expanded as  $F(x)F(y) = 1 - \cos x - \cos y + \cos x \cos y$ , rapidly oscillate except for the constant term 1. Because of this, only the  $\mathcal{F}_{12}$  term given by Eq. (B.2) with all the function  $F$  being replaced with 1 remains as the dominant contribution. As a result, the low-frequency limit of  $\delta_{S^2,dc}$  is given by

$$\begin{aligned} \delta_{S^2,dc} = & -\omega^2 \times 8 \left( \frac{3H_0^2 \Omega_m}{2} \right)^4 \int_0^{\chi_s} \frac{d\chi}{\chi^2} \int_0^\chi \frac{d\chi'}{\chi'^2} \int_0^{\chi'} d\chi_1 \int_0^{\chi'} d\chi_2 \frac{1}{a^2(\chi_1)} \frac{1}{a^2(\chi_2)} \frac{1}{(2\pi)^2} \\ & \times \chi_1^2 \chi_2^2 \int_0^\infty dk_1 \frac{P_\delta(k_1, \chi_1)}{k_1} \int_0^\infty dk_2 \frac{P_\delta(k_2, \chi_2)}{k_2} \propto -\omega^2. \end{aligned} \quad (3.5)$$

Thus, it scales as  $\propto \omega^2$  and is more suppressed than  $\langle S_{\text{Born}}^2 \rangle$ . The straight lines at the low frequency end in both figures are the low-frequency limit of  $\delta_{S^2,dc}$  obtained based on Eq. (3.5). We see that our numerically computed  $\delta_{S^2,dc}$  indeed coincides with the straight lines, which supports the validity of our numerical computations.

We find that  $\delta_{S^2,dc}$  is negative at low frequency. At around  $f = 10^{-12}$  Hz,  $\delta_{S^2,dc}$  turns to



positive for both  $z_s = 1$  and  $z_s = 3$ . However, since the error of the numerical calculation inevitably increases at this specific frequency, we have not been able to confirm the exact value of the frequency at which  $\delta_{S^2, \text{dc}}$  becomes zero. Thus, further investigation is needed for understanding the more precise property of  $\delta_{S^2, \text{dc}}$  at around this frequency.

After turning to be positive side,  $\delta_{S^2, \text{dc}}$  declines in the same way as  $\langle S_{\text{Born}}^2 \rangle$  does. We stopped the numerical calculation beyond  $f = 10^{-7}$  Hz. The reason is that  $\langle (S^{(2)})^2 \rangle_{\text{dc}}$  and  $2 \langle S^{(1)} S^{(3)} \rangle_{\text{dc}}$  are very close in their value except their signature, which causes the cancellation of significant digits in Eq. (2.36) (with all  $K$  being replaced with  $S$ ) and cannot be accurately captured in the numerical computation. It is known that, in geometric optics, the translation invariance of the correlation functions plays a role in this type of cancellation for  $K$  [12–16]. Our calculations suggest that the same reason applies for the cancellation for the variance of  $S$  although we have not been able to prove it mathematically. For frequency larger than  $10^{-7}$  Hz, instead of the direct numerical computation, we use the asymptotic form of  $\delta_{S^2, \text{dc}}$  valid at high frequency in order to extrapolate in the higher frequency region. Writing the matter power spectrum at small scale as the one given by Eq. (3.2), the asymptotic form of  $\delta_{S^2, \text{dc}}$  in the large frequency limit is given by (see appendix C for the derivation)

$$\begin{aligned} \delta_{S^2, \text{dc}} = & \frac{32}{\omega^{\frac{b}{2}-1}} \times \left( \frac{3H_0^2 \Omega_m}{2} \right)^4 \int_0^{\chi_s} \frac{d\chi}{\chi^2} \int_0^\chi \frac{d\chi'}{\chi'^2} \int_0^{\chi'} \frac{d\chi_1}{2\pi} \int_0^{\chi'} \frac{d\chi_2}{2\pi} \frac{1}{a^2(\chi_1)} \frac{1}{a^2(\chi_2)} B(\chi_2) \\ & \times \int_0^\infty dk_1 k_1 P_\delta(k_1, \chi_1) \left[ CI_c + \frac{2}{\chi_2^2 W(\chi_2, \chi_s)} D_1 I_d + CI_e \right] \left( \frac{\chi_2^2 W(\chi_2, \chi_s)}{2} \right)^{\frac{b-2}{2}}, \end{aligned} \quad (3.6)$$

where  $C, D_1, I_c, I_d,$  and  $I_e$  defined in appendix C are independent of  $\omega$ . We find that the index of the scaling  $\delta_{S^2, \text{dc}} \propto \omega^{1-b/2}$  is the same as that of  $\langle S_{\text{Born}}^2 \rangle^{1/2}$ . The dash-dotted line in Fig. 3a and Fig. 3b is obtained by evaluating Eq. (3.6). The fact that these lines nicely coincide with the numerical results in the frequency range where numerical computations are tractable supports that both numerical results and the asymptotic expression (3.6) are evaluated correctly.

Fig. 4 shows the relative magnitude of  $\langle S \rangle^2$  and  $\delta_{S^2, \text{dc}}$  in comparison to  $\langle S_{\text{Born}}^2 \rangle$ . We find that the post-Born effect increases as the frequency becomes larger. When  $f < 10^{-10}$  Hz, the relative magnitude of  $|\delta_{S^2, \text{dc}}|$  is smaller than that of  $\langle S \rangle^2$ , then they get closer until around  $f = 10^{-7}$  Hz. After passing  $f = 10^{-7}$  Hz, the ratio of  $\delta_{S^2, \text{dc}}$  to  $\langle S_{\text{Born}}^2 \rangle$  reaches the maximum ( $\sim 0.05\%$  for  $z_s = 1$  and  $\sim 0.4\%$  for  $z_s = 3$ ).

Let us next investigate the variance of  $K$ . Fig. 5a and Fig. 5b show the correction to  $\langle K_{\text{Born}}^2 \rangle$  in the case where the source redshift is  $z_s = 1$  and  $z_s = 3$ , respectively. Similarly to  $\langle K_{\text{Born}}^2 \rangle$  and  $\langle K \rangle$ , the correction to the variance is suppressed at low frequency and approaches a constant value in the high frequency limit. Interestingly,  $\delta_{K^2, \text{dc}}$  changes the signature at around  $f = 10^{-15}$  Hz from positive to negative as the frequency is increased. Except for the narrow frequency range in which  $\delta_{K^2, \text{dc}}$  flips the sign, the magnitude of  $\delta_{K^2, \text{dc}}$  is of the same order as  $\langle K \rangle^2$  for any frequencies.

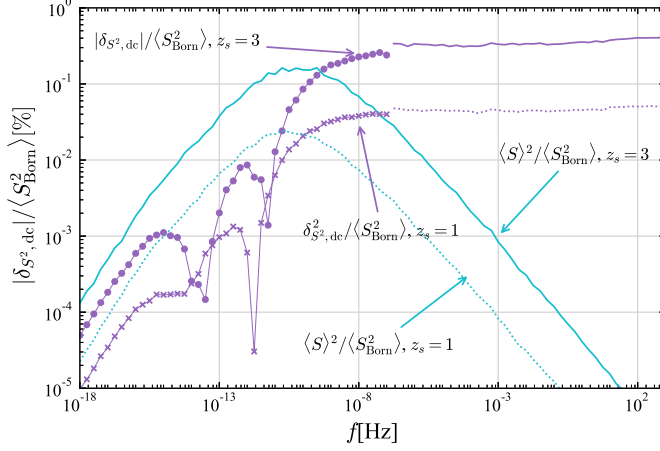


**Figure 4:** This figure shows the relative magnitude of  $|\delta_{S^2,dc}|$  and  $\langle S \rangle^2$  in comparison to  $\langle S^2_{\text{Born}} \rangle$  in the case of  $z_s = 1$  and  $z_s = 3$  in percentile. The purple markers and lines show  $|\delta_{S^2,dc}| / \langle S^2_{\text{Born}} \rangle$ . The cyan solid and dotted lines show  $\langle S \rangle^2 / \langle S^2_{\text{Born}} \rangle$ .  $\delta_{S^2,dc}$  is at most the same order or quite smaller than  $\langle S \rangle^2$  at small frequency ( $f < 10^{-10}$  Hz). In this frequency range,  $|\delta_{S^2,dc}|$  is  $< 0.02\%$  of  $\langle S^2_{\text{Born}} \rangle$  for  $z_s = 1$ , and  $< 0.2\%$  for  $z_s = 3$ . In the higher frequency range ( $f > 10^{-10}$  Hz),  $\langle S \rangle^2$  is suppressed more rapidly than  $\delta_{S^2,dc}$  due to the different asymptotic behavior. Both  $\langle S^2_{\text{Born}} \rangle$  and  $\delta_{S^2,dc}$  are proportional to  $\omega^{-(b-2)/2}$ , and the ratio reaches the maximum.  $\delta_{S^2,dc}$  is  $\sim 0.05\%$  for  $z_s = 1$ , and  $\sim 0.4\%$  for  $z_s = 3$ .

In order to understand the behavior at low frequency, we consider Eq. (B.1). When the frequency is sufficiently small, the dominant contribution to the integrals of  $k_1, k_2$  comes from a small region where both  $k_1$  and  $k_2$  are small (suppressed by  $1/\sqrt{\omega}$ ), i.e., the low frequency behavior is completely determined by the large scale matter power spectrum. Then, taking the single-power law approximation  $P_\delta \propto k^n$  as we have done in 3.1 and substituting it to Eq. (B.1), we can verify that the resultant integrals over  $k_1, k_2$  are convergent. Changing the integration variables by  $k_1 = \sqrt{\omega}\xi_1, k_2 = \sqrt{\omega}\xi_2$  then yields the scaling  $\delta_{K^2,dc} \propto \omega^{2+n}$ , which reproduces the behavior seen in Fig. 5a and Fig. 5b.

In the figure, we also show the geometric optics limit, which is obtained by simply taking the limit  $\omega \rightarrow \infty$  in  $\mathcal{F}_{12}, \mathcal{F}_1$ , and  $\mathcal{F}_2$  given in the Appendix B. The result is given

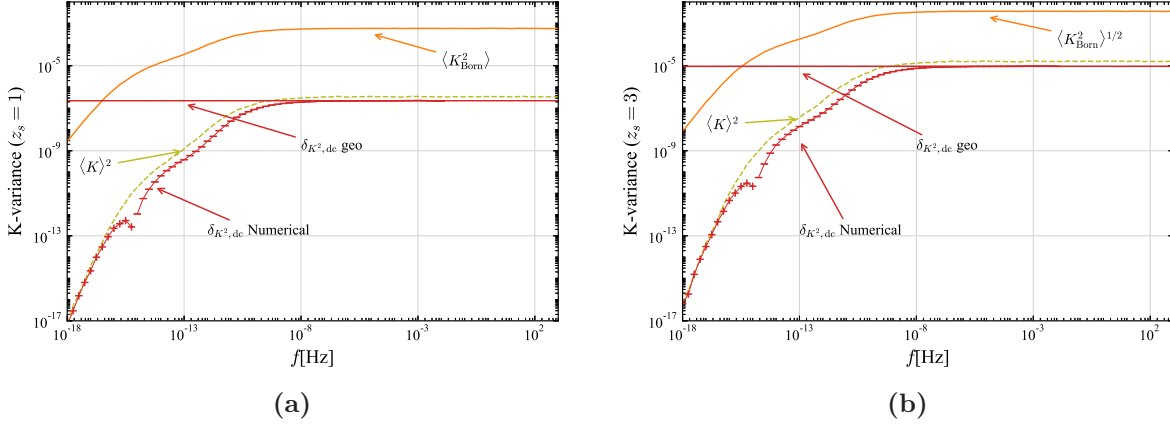


**Figure 5:** The source redshift of (a) is  $z_s = 1$  and (b) is  $z_s = 3$ . The orange solid line and the olive dashed line show  $\langle K_{\text{Born}}^2 \rangle$  and  $\langle K \rangle^2$  respectively. In the same way as  $S$ , the shape of the marker indicates the signature of  $\delta_{K^2,dc}$ . The red solid line shows the geometric optics limit ( $\omega \rightarrow \infty$ ) of  $\delta_{K^2,dc}$ .  $\delta_{K^2,dc}$  is positive at very low frequency and turns to negative at around  $f = 10^{-15}$  Hz. The magnitude of  $\delta_{K^2,dc}$  is roughly the order of  $\langle K \rangle^2$

by

$$\begin{aligned}
\lim_{\omega \rightarrow \infty} \delta_{K^2,dc} = & 16 \left( \frac{3H_0^2 \Omega_m}{2} \right)^4 \int_0^{\chi_s} \frac{d\chi}{\chi^2} \int_0^\chi \frac{d\chi'}{\chi'^2} \int_0^{\chi'} d\chi_1 \int_0^{\chi'} d\chi_2 \frac{1}{a^2(\chi_1)} \frac{1}{a^2(\chi_2)} \frac{1}{(2\pi)^2} \\
& \times \int_0^\infty dk_1 k_1 P_\delta(k_1, \chi_1) \int_0^\infty dk_2 k_2 P_\delta(k_2, \chi_2) \\
& \times \frac{\chi_1^2 \chi_2^4}{8} \left\{ 2W(\chi_1, \chi_s)W(\chi_2, \chi_s) - 2W(\chi', \chi)(W(\chi_1, \chi_s) + W(\chi_2, \chi_s)) \right. \\
& \left. - 2W(\chi_2, \chi_s)W(\chi, \chi_1) - 2W(\chi_1, \chi_s)W(\chi, \chi_2) + 3W(\chi', \chi)W(\chi, \chi_s) \right\}. \tag{3.7}
\end{aligned}$$

As the figure shows, the lines drawn based on the above equation nicely fit with the ones which are obtained by the direct numerical computations without relying on the high frequency approximation.

Fig. 6 is the same as Fig. 4 but for the magnification  $K$ . From this result, we can conclude that  $\langle K \rangle^2 > |\delta_{K^2,dc}|$  is always satisfied. Similar to the phase modulation, the post-Born effect becomes larger at high frequency and the ratio eventually reaches the maximum. We confirmed that  $|\delta_{K^2,dc}|$  is  $< 0.035(0.25)\%$  of  $\langle K_{\text{Born}}^2 \rangle$  for  $z_s = 1(z_s = 3)$  within this frequency range. Because  $\delta_{K^2,dc}$  is negative at relatively higher frequency, the variance should be decreased by this amount from the pure Born approximation.

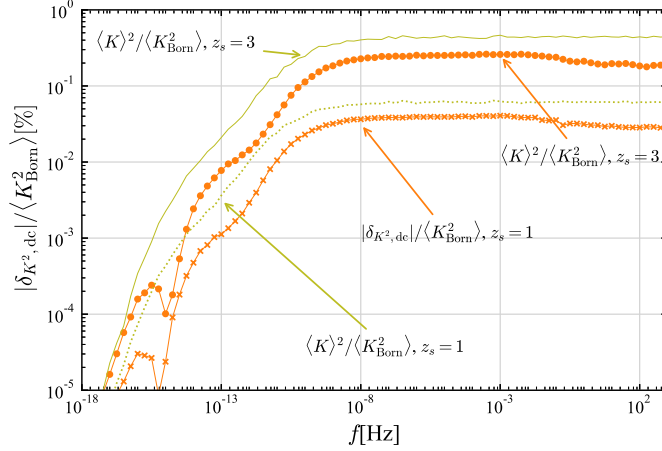


**Figure 6:** This shows the relative magnitude of  $\delta_{K^2,\text{dc}}$  and  $\langle K \rangle$  in comparison to  $\langle K_{\text{Born}}^2 \rangle^{1/2}$ . The orange markers show  $\delta_{K^2,\text{dc}}$  for  $z_s = 1$  and  $z_s = 3$ . When  $f > 10^{-8}$  Hz,  $\delta_{K^2,\text{dc}}$  is 0.035(0.25)% of  $\langle K_{\text{Born}}^2 \rangle^{1/2}$  for  $z_s = 1(z_s = 3)$ . This ratio decreases when the frequency is lower than  $f = 10^{-8}$  Hz.

### 3.4 Shot noise contribution

Up to this point, we have not considered the effect of the shot noise coming from the Poisson distributed stars (or any other dark compact objects) because i) the low frequency GWs are not strongly affected by it and ii) computations are technically difficult for some quantities. However, the shot noise may become important at high frequencies, and in this section we discuss the contribution from the shot noise. At the level of the post-Born approximation, since the variance of  $S, K$  is given by the product of the matter power spectrum, the inclusion of the shot noise contribution yields not only the terms representing purely the shot noise but also the cross terms between the non-shot noise and the shot noise. The evaluation of the latter is beyond the scope of this paper and we will only focus on the former.

Formally, the shot noise is given by adding a constant to the matter power spectrum, namely,

$$P_\delta = \frac{f_p^2}{\bar{n}}, \quad (3.8)$$

where  $\bar{n}$  is the average number density of an individual star and  $f_p$  is the mass fraction of the point mass to total matter density. For simplicity, we ignore the time variation of  $\bar{n}$  due to stellar evolution.

We first evaluate the shot noise contribution to  $\langle S_{\text{Born}}^2 \rangle$  and  $\langle K_{\text{Born}}^2 \rangle$ . Substituting Eq. (3.8) to Eq. (3.3), we can analytically perform the integral over  $k$  by using the formula

$\int_0^\infty \frac{dx}{x^3} (1 - \cos x^2)^2 = 1/(4\pi)$ . Then, we obtain

$$\langle S_{\text{Born}}^2 \rangle_{\text{shot}} = \frac{1}{4} \left( \frac{3H_0\Omega_m}{2} \right)^2 \int_0^{\chi_s} d\chi \frac{1}{a^2(\chi)} \chi^2 W(\chi, \chi_s) \times \omega \frac{f_p^2}{n}. \quad (3.9)$$

Similarly, using the formula  $\int_0^\infty \frac{dx}{x^3} \sin^2 x^2 = 1/(4\pi)$ , we find that  $\langle K_{\text{Born}}^2 \rangle_{\text{shot}} = \langle S_{\text{Born}}^2 \rangle_{\text{shot}}$ . Thus, both the variance of  $S$  and  $K$  under the Born approximation diverge in the high frequency limit. In geometrical optics, the divergence of  $\langle K_{\text{Born}}^2 \rangle_{\text{shot}}$  is nothing but the divergence of the variance of the convergence. Thus, it is caused by the geodesics passing through the point masses, which are extremely rare (mathematically, measure is zero) events. This implies that the divergence of  $\langle K_{\text{Born}}^2 \rangle_{\text{shot}}$  is spurious and realistic  $\langle K_{\text{Born}}^2 \rangle_{\text{shot}}$  becomes zero at  $\omega \rightarrow \infty$ . Yet, it is not clear to us how much this reduction occurs for finite frequency and separate study is needed to clarify this issue. Furthermore, in reality, the point mass approximation breaks down below the size of the stars, which cuts off the power spectrum below that scale.

Let us next investigate the average  $\langle S \rangle$  and  $\langle K \rangle$ . Plugging Eqs. (3.1) and (3.8) into the expression  $\langle S \rangle$  given by Eq. (2.29), we find that the integration over  $k$  diverges logarithmically at large  $k$ . Hence, we need to introduce the cutoff wavenumber  $k_c$  which physically represents the inverse of the size of the stars. With this cutoff, we can perform the integration over  $k$  and the result is given by

$$\langle S \rangle_{\text{shot}} = 2 \left( \frac{3H_0\Omega_m}{2} \right)^2 \int_0^{\chi_s} d\chi \int_0^\chi d\chi' \frac{\chi'^2}{\chi^2} \frac{1}{a^2(\chi')} \frac{1}{4\pi} \text{Cin} \left( k_c^2 \frac{\chi'^2 W(\chi', \chi)}{\omega} \right) \times \omega \frac{f_p^2}{n} \quad (3.10)$$

where  $\text{Cin}(x)$  is the cosine integral defined as  $\text{Cin}(x) = \int_0^x dt \frac{1 - \cos t}{t}$ . When  $x$  is sufficiently large, the cosine integral is approximated as  $\text{Cin}(x) \approx \log(e^\gamma x)$ , where  $\gamma$  is Euler's constant. We usually consider the case where  $\chi_s$  takes the cosmological distance ( $\chi_s \approx 1/H_0$ ). In this specific case, we can further approximate this expression to

$$\langle S \rangle_{\text{shot}} \sim \frac{1}{\pi} \left( \frac{3H_0\Omega_m}{2} \right)^2 \int_0^{\chi_s} d\chi \int_0^\chi d\chi' \frac{\chi'^2}{\chi^2} \frac{1}{a^2(\chi')} \times \omega \frac{f_p^2}{n} \log \left( \frac{k_c}{\sqrt{H_0\omega}} \right). \quad (3.11)$$

As for  $\langle K \rangle$ , the integral over  $k$  does not diverge and we can practically take  $k_c \rightarrow \infty$ . Then, the result is given by

$$\langle K \rangle_{\text{shot}} = -\frac{1}{4} \left( \frac{3H_0\Omega_m}{2} \right)^2 \int_0^{\chi_s} d\chi \int_0^\chi d\chi' \frac{\chi'^2}{\chi^2} \frac{1}{a^2(\chi')} \times \omega \frac{f_p^2}{n}. \quad (3.12)$$

We finally evaluate the post-Born correction to the variance. Due to the same reason as  $\langle S \rangle_{\text{shot}}$ , the integral for  $\delta_{S^2, \text{dc}}$  diverges and the variance depends on the cutoff  $k_c$ . According to (B.10), when  $k_1$  and  $k_2$  are large enough, the integrand behaves as  $\frac{1}{k_1 k_2}$  due to the cancellation by oscillations. In other words, it is possible to make the following approximation

$$\left[ \frac{1}{k_1 k_2} \mathcal{F}_{S,12} - \frac{1}{k_1^2} \mathcal{F}_{S,1} - \frac{1}{k_2^2} \mathcal{F}_{S,2} \right] \sim -\frac{1}{2k_1 k_2} \left( 1 - \cos \left( \frac{\chi_1^2 W(\chi_1, \chi_s)}{2\omega} k_1^2 \right) \right) \left( 1 - \cos \left( \frac{\chi_2^2 W(\chi_2, \chi_s)}{2\omega} k_2^2 \right) \right) \quad (3.13)$$

when  $k_1$  and  $k_2$  are sufficiently large. Using this approximation as well as other simplifications used in the computation of  $\langle S \rangle_{\text{shot}}$ , we obtain

$$\begin{aligned} \delta_{S^2, \text{dc, shot}} \sim & -8 \left( \frac{3H_0^2 \Omega_m}{2} \right)^4 \int_0^{\chi_s} \frac{d\chi}{\chi^2} \int_0^\chi \frac{d\chi'}{\chi'^2} \int_0^{\chi'} d\chi_1 \int_0^{\chi'} d\chi_2 \frac{1}{a^2(\chi_1)} \frac{1}{a^2(\chi_2)} \frac{1}{(2\pi)^2} \chi_1^2 \chi_2^2 \\ & \times \omega^2 \left( \frac{f_p^2}{\bar{n}} \right)^2 \left( \log \left[ \frac{k_c}{\sqrt{H_0 \omega}} \right] \right)^2. \end{aligned} \quad (3.14)$$

As for  $\delta_{K^2, \text{dc}}$ , it does not diverge even if we take  $k_c \rightarrow \infty$ . Taking this limit, the formal expression is given by

$$\begin{aligned} \delta_{K^2, \text{dc, shot}} = & 16 \left( \frac{3H_0^2 \Omega_m}{2} \right)^4 \int_0^{\chi_s} \frac{d\chi}{\chi^2} \int_0^\chi \frac{d\chi'}{\chi'^2} \int_0^{\chi'} d\chi_1 \int_0^{\chi'} d\chi_2 \frac{1}{a^2(\chi_1)} \frac{1}{a^2(\chi_2)} \frac{1}{(2\pi)^2} \\ & \times \int_0^\infty dk_1 \int_0^\infty dk_2 \left[ \frac{1}{k_1 k_2} \mathcal{F}_{K,12} - \frac{1}{k_1^2} \mathcal{F}_{K,1} - \frac{1}{k_2^2} \mathcal{F}_{K,2} \right] \times \omega^2 \frac{f_p^2}{\bar{n}}. \end{aligned} \quad (3.15)$$

The definition of  $\mathcal{F}_{K,12}$ ,  $\mathcal{F}_{K,1}$ ,  $\mathcal{F}_{K,2}$  is given in Appendix B. We have not been able to find an analytic method to approximately compute the integration over  $k_1, k_2$  because it requires careful analytical treatment. Although it is, in principle, possible to compute the integral numerically, it turned out to be quite complicated to achieve it. This arises from the fact that the expression is highly oscillatory at large  $k$ .

In order to calculate the shot noise effect, we use the relation  $\bar{\rho} \Omega_m f_p = m_p \bar{n}$ , and  $H_0^2 = \frac{8\pi G}{3} \bar{\rho}$ . For simplicity, we assume that all stars have the same mass ( $m_p = 0.5 M_\odot$ ) and take  $f_p = 0.009$  as a fiducial value which is consistent with the measured abundance of stars [20]. Since the cutoff scale  $k_c$  represents the size of the stars, we choose  $k_c = 4 \times 10^{13} \text{ hMpc}^{-1} (\sim 10^{-6} \text{ km}^{-1})$ .

We show the effect of the shot noise on  $\langle S_{\text{Born}}^2 \rangle$ ,  $\langle S \rangle$ ,  $\delta_{S^2, \text{dc}}$  in Fig. 7a and Fig. 7b, and  $\langle K_{\text{Born}}^2 \rangle$  and  $\langle K \rangle$  in Fig. 8a and Fig. 8b, respectively. We do not show the result of  $\delta_{K^2, \text{dc, shot}}$  in this paper due to the reason explained above.

As shown in Fig. 7a and Fig. 7b, the shot noise effect manifests itself at  $f \sim 10^0$  Hz for  $\langle S_{\text{Born}}^2 \rangle$  and keeps increasing ( $\langle S_{\text{Born}}^2 \rangle \propto \omega$ ).  $\langle S \rangle^2$  and  $\delta_{S^2, \text{dc}}$  show the almost similar behavior to  $\langle S_{\text{Born}}^2 \rangle$ , but they are proportional to  $\omega^2$ . Therefore, the post-Born effect could become more important than  $\langle S_{\text{Born}}^2 \rangle$  at very high frequencies. In addition to this, the distance to the source is another factor to enhance the post-Born effect. From the figure, we see that at the higher frequency end of the current detection limit ( $\sim 1000$  Hz),  $\delta_{S^2, \text{dc}}$  is 2% of  $\langle S_{\text{Born}}^2 \rangle$  for  $z_s = 1$  and 14% for  $z_s = 3$ . The Born approximation is still valid, but the post-Born effect will become non-negligible beyond this frequency and the redshift.

As far as  $\langle S \rangle$  is concerned, we may be able to detect  $\langle S \rangle$  as this is purely caused by the post-Born effect. The detectability regarding  $\langle S \rangle$  and  $\langle K \rangle$  is discussed in the next section. Before considering the shot noise effect on the magnification, it is constructive to mention the usage of the shot noise as a probe of the point-like objects. The amplitude of  $\langle S \rangle$  under the shot noise effect is determined by not only  $f_p$  and  $\bar{n}$ , which represents the stellar mass

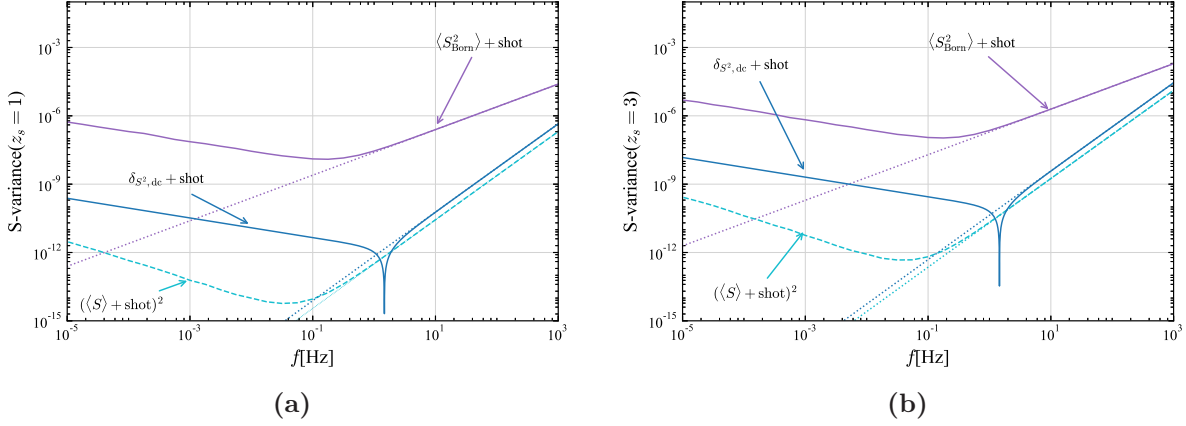


**Figure 7:** The shot noise effect on the phase modulation  $S$ . The source redshift is  $z_s = 1$  and  $z_s = 3$  for (a) and (b) respectively. The purple solid line shows the Born approximation. The cyan and the blue line show  $\langle S \rangle^2$  and  $\delta_{S^2,dc}$ . The dotted lines show the pure shot noise effect for all cases. In both figures, the shot noise effect becomes dominant at around  $f \sim 10^0$  Hz for the Born approximation. On the other hand, the average of  $S$  is affected by the shot noise at around  $f \sim 10^{-2}$  Hz. The magnitude of  $\delta_{S^2,dc}$  and  $\langle S \rangle^2$  is of the same order under the shot noise effect and both have the same frequency dependence ( $\propto \omega^2$ ). Since  $\langle S_{\text{Born}}^2 \rangle \propto \omega$ , the post-Born effect grows faster than the Born result within this frequency range. The signature of  $\delta_{S^2,dc}$  changes when the shot noise effect manifests itself. This can be seen as a sudden decrease and increase of the magnitude of  $\delta_{S^2,dc}$  at  $f = 6 \times 10^{-1}$  [Hz]. At the high detectable frequency end of GWs ( $f \leq 1000$  Hz), the post-Born effect is  $\leq 2\%$  for  $z_s = 1$  and  $\leq 14\%$  for  $z_s = 3$ .

fraction and the average mass of an individual point mass, but also the cutoff scale  $k_c$ . Provided that  $\langle S_{\text{Born}}^2 \rangle$  does not depend on  $k_c$ , we can use the observed data of  $\langle S \rangle$  to infer  $k_c$ . The shot noise is not only caused by the stars but also by other compact objects such as the black holes (BHs). Because BHs have quite large  $k_c$ , which would correspond to the size of the event horizon, compared to that of stars, BHs will yield different magnitudes of  $\langle S_{\text{Born}}^2 \rangle$  and  $\langle S \rangle$  from those produced by stars. This consideration raises an intriguing possibility that the main constituent of the shot noise may be determined by measuring both  $\langle S_{\text{Born}}^2 \rangle$  and  $\langle S \rangle$ .

Fig. 8a and Fig. 8b show the shot noise effect on the magnification  $K$ . The shot noise effect only appears at  $f \geq 10^4$  Hz. When the frequency is lower than this value, both  $\langle K_{\text{Born}}^2 \rangle$  and  $\langle K \rangle$  are constant. Just like  $S$ ,  $\langle K \rangle^2 (\propto \omega^2)$  increases faster than  $\langle K_{\text{Born}}^2 \rangle (\propto \omega)$  under the shot noise effect as the GW frequency is increased. As far as the current detectable frequency is concerned,  $\langle K \rangle^2$  is 0.06% of  $\langle K_{\text{Born}}^2 \rangle$  for  $z_s = 1$  and 0.45% for  $z_s = 3$ . If  $\delta_{K^2,dc}$  turns out to be the same order of magnitude as  $\langle K \rangle^2$ , then the same thing could be applied to  $\delta_{K^2,dc}$ , that the shot noise effect only becomes important at



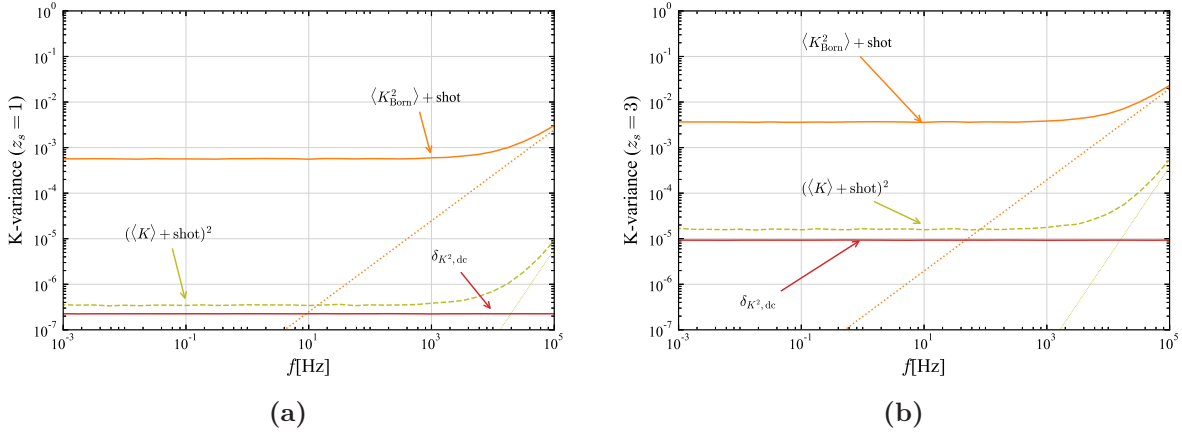


**Figure 8:** The shot noise effect on the magnification is shown in these figures ((a) for  $z_s = 1$  and (b) for  $z_s = 3$ ). The red line and the olive line show  $\langle K_{\text{Born}}^2 \rangle$  and  $\langle K \rangle$  respectively. The dotted lines are the pure shot noise effect. Because of the difference of the dependence on  $\omega$  ( $\langle K_{\text{Born}}^2 \rangle \propto \omega$  and  $\langle K \rangle^2 \propto \omega^2$ ), the post-Born effect eventually overcomes the Born result. However, this only happens at a very high frequency ( $f \geq 10^4$  Hz). Therefore, it is safe to say that the shot noise is subdominant at a low frequency. At the detectable frequency,  $\langle K \rangle^2$  is  $\leq 0.06\%$  for  $z_s = 1$  and  $\leq 0.45\%$  for  $z_s = 3$ . Although we do not show  $\delta_{K^2, \text{dc}, \text{shot}}$  due to the difficulty of the calculation, we suspect that it exceeds  $\langle K \rangle^2$ .

$f \geq 10^4$  Hz. Our numerical results support this idea as  $\langle K \rangle^2 > |\delta_{K^2, \text{dc}}|$  is always satisfied within the frequency range discussed in this paper. Therefore, we expect the shot noise effect on  $\delta_{K^2, \text{dc}}$  is as small as  $\langle K \rangle^2$  although reliable numerical study is needed to draw a definite conclusion.

## 4 Discussion

In this section, we summarize our main findings and discuss the possibility of the applications and the detectability of the post-Born effect.

### 4.1 Validity of the Born approximation

In Table 1, we show the magnitude of the post-Born corrections relative to the Born approximation calculated in this paper. We find that the amount of the corrections is not more than a few percent of the Born approximation for both  $S$  and  $K$  when  $f < 10^1$  Hz. Therefore, we can safely say that the theoretical error caused by excluding the post-Born effect is at least two orders of magnitude smaller than the Born approximation. However, when the frequency is high  $f \geq 10^3$  Hz and the source redshift is also large ( $z_s = 3$ ), we have to be cautious about the interpretation of  $\langle S_{\text{Born}}^2 \rangle$ . As shown in Table 1,  $\langle S \rangle$  could become

25% of  $\langle S_{\text{Born}}^2 \rangle^{1/2}$  and  $\delta_{S^2, \text{dc}}$  could become 14% of  $\langle S_{\text{Born}}^2 \rangle$  when  $z_s = 3$  and  $f = 10^3$  Hz are satisfied. This is due to the shot noise effect, that  $S$  and  $K$  are heavily dependent upon the mass, fraction, and the size of the shot noise constituent. Since  $P_\delta = f_p^2/\bar{n} \propto f_p m_p$  and  $m_p = 0.5M_\odot$ , the amplitude of  $P_\delta$  increases by a factor of 100 if we replace  $m_p = 0.5M_\odot$  with  $m_p = 50M_\odot$  while having  $f_p$  fixed. This corresponds to a scenario in which the fifty solar mass black holes as part of dark matter are as prevalent as the stellar components. This scenario has attracted great interest recently after observations of such massive black holes by the GW experiments. It is under active investigation whether the abundance of primordial black holes comparable to  $f_p \simeq 0.01$  is consistent with existing observations [21]. GL of GWs studied in this paper provides an alternative path to test this possibility (see also [10]). According to Eqs. (3.9), (3.11), (3.12), (3.14), and (3.15),  $\langle S_{\text{Born}}^2 \rangle$  and  $\langle K_{\text{Born}}^2 \rangle$  are proportional to  $f_p m_p$  whereas  $\langle S \rangle^2$ ,  $\langle K \rangle^2$ ,  $\delta_{S^2, \text{dc}}$ , and  $\delta_{K^2, \text{dc}}$  are proportional to  $f_p^2 m_p^2$ . Thus,  $\langle S \rangle / \langle S_{\text{Born}}^2 \rangle^{1/2}$  and  $\langle K \rangle / \langle K_{\text{Born}}^2 \rangle^{1/2}$  become 10 times bigger while  $\delta_{S^2, \text{dc}} / \langle S_{\text{Born}}^2 \rangle$  and  $\delta_{K^2, \text{dc}} / \langle K_{\text{Born}}^2 \rangle$  become 100 times bigger than the values shown in Table 1 at a high frequency. In this case, the post-Born effect dominates over the Born approximation and the approximation seems to be no longer useful. However, we have to emphasize that this has to be caused by rare events in which the shot noise constituent is very close to the line of sight. When the point like object is on the line of sight, the incoming GWs are affected so much that the observed signal would be strongly lensed. Though these events are rare, the overall ensemble average is dominated by them due to the strong perturbation on the amplitude and phase. In reality, these rare events are removed when they are identified as strong lensing. However, we need to determine the probability distribution of each event to incorporate how much the reduction of the ensemble average is expected by removing rare events. Investigating this is beyond the scope of this paper and needs to be addressed in the future.

## 4.2 Average as an additional probe

We find that the ensemble average of  $K$  and  $S$  is no longer zero at the level of the post-Born approximation. As shown in Table 1,  $\langle K \rangle$  is less than 6% of  $\langle K_{\text{Born}}^2 \rangle^{1/2}$  across all frequency range considered in this paper, while  $\langle S \rangle$  could become more than 10% of  $\langle S_{\text{Born}}^2 \rangle^{1/2}$  in some case. Since the average depends on the matter power spectrum differently from the variance, we may use this quantity as an additional quantity to probe the matter power spectrum. As for  $\langle K \rangle$ , the more interesting result could be extracted by either differentiating it with respect to  $f$  or subtracting two values of  $\langle K \rangle$  measured at the different frequency  $f_1$  and  $f_2$ . The subtraction or differentiation of  $K$  allows us to remove the effect of the geometric optics and gives the pure frequency dependence of  $\langle K \rangle$ . As far as  $\langle S \rangle$  is concerned, we should focus on the high frequency region ( $f \geq 10^0$  Hz) where the shot noise effect is dominant. This is due the fact that  $\langle S \rangle$  would be too small to detect ( $\langle S \rangle$  is only 0.2% of  $\langle S_{\text{Born}}^2 \rangle^{1/2}$  at  $f = 10^{-2}$  Hz) when the shot noise effect is still hidden. Once the shot noise effect manifests itself,  $\langle S_{\text{Born}}^2 \rangle$  and  $\langle S \rangle$  show almost the same

	$f \leq 10^{-2}$ Hz	$10^{-2} \leq f \leq 10^1$ Hz	$10^1 \leq f \text{ Hz} \leq 10^3$ Hz
$\langle K \rangle / \langle K_{\text{Born}}^2 \rangle^{1/2}$	$\leq 2.4(6)\%$		
$\langle S \rangle / \langle S_{\text{Born}}^2 \rangle^{1/2}$	$\leq 1.5(4)\%$	$\leq 1(3)\%$	$\leq 8(25)\%$
$\delta_{K^2, \text{dc}} / \langle K_{\text{Born}}^2 \rangle$	$\leq 0.035(0.25)\%$		
$\delta_{S^2, \text{dc}} / \langle S_{\text{Born}}^2 \rangle$	$\leq 0.05(0.4)\%$	$\leq 0.02(0.2)\%$	$\leq 2(14)\%$

**Table 1:** The post-Born corrections to  $\langle S_{\text{Born}}^2 \rangle$  and  $\langle K_{\text{Born}}^2 \rangle$  for  $z_s = 1(3)$ . Each value represents the maximum of corrections to the Born approximation within an assigned frequency range. When the frequency is low ( $f \leq 10^{-2}$  Hz),  $\langle S \rangle / \langle S_{\text{Born}}^2 \rangle^{1/2}$  is a decreasing function of  $f$ . As shown in Fig.4, the maximum of  $\langle S \rangle$  is realized at  $f = 10^{-11} \sim 10^{-10}$  Hz. For this reason, the value of  $\langle S \rangle / \langle S_{\text{Born}}^2 \rangle^{1/2}$  listed in this table is measured at  $f = 3 \times 10^{-11}$  Hz. At  $f = 10^{-2}$  Hz,  $\langle S \rangle$  is only 0.2% of  $\langle S_{\text{Born}}^2 \rangle^{1/2}$  even if the redshift is  $z_s = 3$ .

but slightly different dependence on it.

Note that the shot noise effect is contaminated by the strong lensing and the analysis needs to be done carefully. Despite this non-trivial issue, the fact that  $\langle S \rangle$  and  $\langle S_{\text{Born}}^2 \rangle$  are not related to each other in a trivial way suggests the possibility to explore the nature of the shot noise (size, mass, fraction) by combining the results from  $\langle S_{\text{Born}}^2 \rangle$  and  $\langle S \rangle$ . The obtained properties of the shot noise may be compared with those of stars inferred by other astronomical observations to test whether the source causing the shot noise in the gravitational lensing of GWs is stars or other type of compact objects that have not been detected by non-GW observations.

It is also important to mention that, according to our formulation,  $\langle S \rangle$  is always positive. If the negative value of  $\langle S \rangle$  is detected, that means an indication of the presence of something outside the lensing effect. It could mean the presence of new matter that interacts with gravity in an unusual way or the violation of GR, which could lead to new physics.

### 4.3 Detectability of the post-Born effect

In [22], it is suggested that the amplitude and phase fluctuation can be measured with an accuracy of  $1/SNR$ , where  $SNR$  is the signal-to-noise ratio. According to [10], the accuracy of the measurement is improved by combining many gravitational events. In [10], it was argued that the required accuracy is written as  $\sim (2/N_{\text{event}})^{1/4}(1/SNR)$ , which yields  $N_{\text{event}} = 3 \times 10^5$  as the number of the GW events (with  $SNR = 50$ ) necessary for detecting the lensing signal. We would like to perform the similar estimation of  $N_{\text{event}}$  required to detect the post-Born effect.

To this end, let us first consider the average of  $K$  and  $S$ . Since our purpose is to

estimate  $N_{\text{event}}$  by the back-of-the-envelope calculations, we will consider the following toy model which simplifies the situation without losing the essential point. Suppose we have succeeded in inferring the source parameters and hence the unlensed waveform from the GW measurement. Then, the residual signal, which we denote by  $s$ , which remains after subtracting the unlensed waveform from the measured waveform consists of the uncertainties  $n$  of the unlensed waveform and the lensing signal  $X$ , namely

$$s_{X,i} = n_i + X_i, \quad (4.1)$$

where  $i$  labels the GW events, and  $X$  takes either  $S$  and  $K$ . For simplicity, we assume that both  $n_i$  and  $X_i$  are Gaussian random variables and each GW event is independent of others. In this case, the ensemble average of the quantities computed from  $n_i$  and  $X_i$  are given by

$$\langle n_i n_j \rangle = \left( \frac{1}{SNR} \right)^2 \delta_{ij}, \quad (4.2)$$

$$\langle X_i \rangle = \mu_X, \quad (4.3)$$

$$\langle X_i X_j \rangle = \sigma_X^2 \delta_{ij} + \mu_X^2, \quad (4.4)$$

$$\langle n_i X_j \rangle = 0. \quad (4.5)$$

Here,  $\mu_X$  and  $\sigma_X$  are the values of both the average and the standard deviation of the phase modulation and the magnification. All the other quantities can be computed from the combination of these relations. The first relation  $\langle n_i n_j \rangle = \delta_{ij}/SNR^2$  is about the accuracy of detecting the phase and magnification fluctuation mainly discussed in [22].

In reality, we are only able to detect the finite number of GW events. Thus, it is convenient to introduce the estimator of the average  $\mu_X$  defined as

$$\mathcal{E}_\mu = \frac{1}{N_{\text{event}}} \sum_{i=1}^{N_{\text{event}}} s_{X,i}. \quad (4.6)$$

This quantity is the approximated version of the ensemble average and taking  $N_{\text{event}} \rightarrow \infty$  reproduces  $\mu_X$ . Indeed, computing the average and the variance of  $\mathcal{E}_\mu$ , we obtain

$$\langle \mathcal{E} \rangle_\mu = \mu_X, \quad (4.7)$$

$$\langle \mathcal{E}_\mu^2 \rangle - \langle \mathcal{E}_\mu \rangle^2 \sim \left( \frac{1}{SNR} \right)^2 \frac{1}{N_{\text{event}}}. \quad (4.8)$$

It is important to mention that we have used the assumption  $1/SNR \gg \mu_X, \sigma_X$  to derive the second equation. This result shows that  $\mathcal{E}_\mu$  fluctuates around  $\mu_X$  with the fluctuation width of about  $\left( \frac{1}{SNR} \right) \frac{1}{\sqrt{N_{\text{event}}}}$ . In order to confidently conclude that the average is nonzero,  $\mu_X > \left( \frac{1}{SNR} \right) \frac{1}{\sqrt{N_{\text{event}}}}$  needs to be satisfied. Using this restriction, we can estimate that  $N_{\text{event}} \sim \left( \frac{1}{SNR} \right)^2 \frac{1}{\mu_X^2}$  is at least necessary to detect the average of  $K$  and  $S$ . As shown

in the previous section,  $\langle S \rangle$  is only 0.2% of  $\langle S_{\text{Born}}^2 \rangle^{1/2} \sim \mathcal{O}(10^{-3})$  at  $f = 10^{-2}$  Hz and  $z_s = 3$ , so  $\langle S \rangle$  is of order  $\mathcal{O}(10^{-7})$ . In this case, we find  $N_{\text{event}} \sim 4 \times 10^{10}$  with  $SNR = 50$ , which may be too large to be achieved in the near future. However, when the frequency of GWs is larger, for instance  $f = 100$  Hz, the shot noise effect becomes dominant and  $\langle S \rangle$  is enhanced as much as  $\mathcal{O}(10^{-4})$ . In this case, we only need  $N_{\text{event}} = 4 \times 10^4$  for  $\langle S \rangle$ , which is, interestingly enough, smaller than the required GW events for detecting  $\langle S_{\text{Born}}^2 \rangle^{1/2}$ . Thus, although it only applies to high frequency GWs, the value of  $N_{\text{event}}$  necessary to detect  $\langle S_{\text{Born}}^2 \rangle^{1/2}$  would be already sufficient to observe  $\langle S \rangle$ .

Next, we consider the detectability of  $\langle K \rangle$ . The typical magnitude of  $\langle K \rangle$  at the detectable frequency is  $\mathcal{O}(10^{-4})$  (it could be  $\mathcal{O}(10^{-3})$  if the source redshift is  $z_s = 3$ ). We can use the same formula and obtain the number  $N_{\text{event}} = 4 \times 10^4$  with  $SNR = 50$  for observing  $\langle K \rangle$ , which is again the same or smaller than the requirement for detecting  $\langle K_{\text{Born}}^2 \rangle^{1/2}$ . This result suggests that detecting the average of  $K$  and  $S$  could be more easily achieved than the detection of the variance, even though the average is intrinsically the post-Born effect and it is intuitively harder to detect than the quantities whose leading order terms appear in the Born approximation. Therefore, we can measure the average with the same detection cost as the variance, which would become a huge advantage in probing the matter power spectrum as they are independent quantities and show different, non-trivial frequency dependence.

Now, we consider the detectability of the post-Born variance. In this case, we need at least two independent measurements of the residual for the same GW event. The reason for this is that we cannot distinguish the lensing signal from the uncertainty associated with the unlensed waveform by using only one measurement. For this purpose, we denote the signals from two different measurements (1 and 2) to be  $s_{X,1,i} = n_{1,i} + X_i$ ,  $s_{X,2,i} = n_{2,i} + X_i$  and assume that one measurement noise is independent of the other's  $\langle n_{1,i} n_{2,j} \rangle = 0$ . The detectability is calculated in the same way above by introducing the estimator of the variance

$$\mathcal{E}_{\sigma_X^2} = \frac{1}{N_{\text{event}}} \sum_{i=1}^{N_{\text{event}}} s_{X,1,i} s_{X,2,i} - \frac{1}{N_{\text{event}}^2} \sum_{i=1}^{N_{\text{event}}} s_{X,1,i} \sum_{j=1}^{N_{\text{event}}} s_{X,2,j}. \quad (4.9)$$

From this expression, we obtain the expressions of the ensemble average of  $\mathcal{E}_{\sigma_X^2}$ :

$$\langle \mathcal{E}_{\sigma_X^2} \rangle = \sigma_X^2, \quad (4.10)$$

$$\langle \mathcal{E}_{\sigma_X^2}^2 \rangle - \langle \mathcal{E}_{\sigma_X^2} \rangle^2 \sim \left( \frac{1}{SNR} \right)^4 \frac{1}{N_{\text{event}}}. \quad (4.11)$$

The interpretation of this result is exactly the same as  $\mathcal{E}_{\mu_X}$  that  $\mathcal{E}_{\sigma_X^2}$  fluctuates around  $\sigma_X^2$  with the width of about  $\left( \frac{1}{SNR} \right)^2 \frac{1}{\sqrt{N_{\text{event}}}}$ . Since the variance of  $S$  and  $K$  are written as  $\sigma_X^2 = \langle X_{\text{Born}}^2 \rangle + \delta_{X^2,\text{dc}}$ , measuring  $\delta_{X^2,\text{dc}}$  requires the satisfaction of the condition  $|\delta_{X^2,\text{dc}}| > \left( \frac{1}{SNR} \right)^2 \frac{1}{\sqrt{N_{\text{event}}}}$ . In the coming decades, the signal-to-noise ratio is expected

to reach  $SNR > 100$  [23]. Considering the previous results that  $\delta_{K^2,dc} \sim \mathcal{O}(10^{-6})$  and  $\delta_{S^2,dc} \sim \mathcal{O}(10^{-8} - 10^{-10})$  (the shot noise effect is ignored), we can estimate that the necessary number of the GW events (with  $SNR = 100$ ) is  $N_{\text{event}} = 1 \times 10^8$  for  $\delta_{S^2,dc}$  and  $N_{\text{event}} = 1 \times 10^4$  for  $\delta_{K^2,dc}$ , respectively. At first glance, the required number for detecting  $\delta_{K^2,dc}$  seems to be more achievable than that for  $\delta_{S^2,dc}$ . However, there are two important caveats that may hinder this naive expectation. i) separating the post-Born contributions from the observed signal requires the precise knowledge of the Born approximation, which is itself difficult due to the smallness of the post-Born corrections and ii) the information extracted from the magnification would be just a frequency independent, constant value that does not explicitly contain the information about the small scale matter power spectrum. In order to make use of  $\delta_{K^2,dc}$  effectively, we need to eliminate the constant magnification under which our target quantity is buried. Within the range of the Born approximation, this is partially studied in [19], where the universal relation between  $\langle S_{\text{Born}}^2 \rangle$  and  $\langle K_{\text{Born}}^2 \rangle$ , namely  $\langle K_{\text{Born}}^2(2f) \rangle - \langle K_{\text{Born}}^2(f) \rangle = \langle S_{\text{Born}}^2(f) \rangle$ , suggests that the same degree of information is encoded in  $\langle K_{\text{Born}}^2 \rangle$  and can be extracted when it is properly treated. We expect that the same logic applies to  $\delta_{K^2,dc}$  that the tight measurement requirement for  $\delta_{S^2,dc}$  ( $N_{\text{event}} = 1 \times 10^8$ ) with  $SNR = 100$  is also necessary for extracting the meaningful information from  $\delta_{K^2,dc}$ . When the shot noise is included,  $\delta_{S^2,dc}$  could become more than  $\mathcal{O}(10^{-7})$  within the detectable frequency (10~1000 Hz) and the required GW events reduce to less than  $N_{\text{event}} = 1 \times 10^6$  with  $SNR = 100$ . However, the difficulty of separating  $\delta_{S^2,dc}$  from  $\langle S_{\text{Born}}^2 \rangle$  prevents us from measuring  $\delta_{S^2,dc}$  with this requirement just like the previous argument. Therefore, even though the improvement of the GW detectors are promising, we may need more time to detect the post-Born effect on the variance.

#### 4.4 Non-Gaussianity

In calculating  $K$  and  $S$ , we have assumed that the power spectrum is Gaussian and then ignored the terms containing the bispectrum and the trispectrum. For the post-Born variance, we find that  $\delta_{S^2,dc}$  and  $\delta_{K^2,dc}$  (i.e., contribution from the Gaussian matter fluctuations) change its signature as the frequency of GWs sweeps across the matter power spectrum at the corresponding Fresnel scale. However, understanding the specific behavior of only  $\delta_{S^2,dc}$  ( $\delta_{K^2,dc}$ ) is incomplete because the contribution of the bispectrum (and the trispectrum) to the variance might be comparable to  $\delta_{S^2,dc}$  ( $\delta_{K^2,dc}$ ). We have derived the bispectrum contribution to  $K$  (and  $S$  by replacing  $\sin$  with  $1 - \cos$ ) in Eq. (2.41) and the trispectrum contribution in Eqs. (2.43) and (2.42), respectively. Once the concrete shape of the bispectrum and the trispectrum are provided, those equations may be used to evaluate the impact of non-Gaussianity on the variance of the lensing signal. By doing this, we are able to clarify how much information of non-Gaussianity is encoded in  $\delta_{S^2,dc}$  and  $\delta_{K^2,dc}$ . In principle, the measurement of these quantities gives a novel way to probe the non-Gaussianity of the matter fluctuations on small scales from the GW observations.

Technically, as we discussed in the previous section, the numerical computation of the variance beyond the Born approximation is difficult due to the cancellation of two large



terms. We expect that such difficulty does not arise in the non-Gaussian sector since the bispectrum contribution has different power dependence on the gravitational potential from the trispectrum. We leave the investigation of contribution to  $S$  and  $K$  from the non-Gaussianity of the matter fluctuations for future work.

## 5 Conclusion

In this paper, we have investigated the weak lensing of GWs beyond the Born approximation by including the higher order terms in the gravitational potential  $\Phi$ . To this end, we first started with a new formulation for the equation governing the GL of GWs. Instead of choosing  $F$  as a fundamental variable, which is called the amplification factor and defined as the ratio of the lensed waveform to unlensed one, we introduced a new variable  $J$  defined as  $F = e^{i\omega J}$ . This process allows us to partially include the non-linear effect of the gravitational potential and reduces the complexity of calculating the terms beyond the Born approximation. We then derived the expression of the phase modulation  $S$  and the magnification  $K$  up to third order in  $\Phi$  and calculated the average and variance up to fourth order in  $\Phi$ . To evaluate the validity of the Born approximation, we numerically computed  $\langle S \rangle, \langle K \rangle, \delta_{K^2, \text{dc}}, \delta_{S^2, \text{dc}}$  by using the matter power spectrum obtained by the phenomenological halo model. We found that, at the level of the post-Born approximation,  $\langle S \rangle$  and  $\langle K \rangle$  are no longer zero. Based on our calculation, the magnitude of  $\langle S \rangle$  and  $\langle K \rangle$  without the shot noise effect is  $\leq 4\%$  and  $\leq 6\%$  of  $\langle S_{\text{Born}}^2 \rangle^{1/2}$  and  $\langle K_{\text{Born}}^2 \rangle^{1/2}$ , respectively. The inclusion of the shot noise enhances  $\langle S \rangle$  as much as 25% of  $\langle S_{\text{Born}}^2 \rangle^{1/2}$  when the source is located at  $z = 3$  and the frequency of GWs is at the upper limit of the current detectable range (1000[Hz]). We then estimated that the number of GW events necessary for detecting  $\langle S \rangle$  and  $\langle K \rangle$  including the shot noise effect, and have shown that it could be as small as  $N_{\text{event}} = 4 \times 10^4$  with  $\text{SNR} = 50$  when the frequency of GWs is within the current detectable range (10~1000 Hz). Interestingly, this number is even smaller than the necessary events for observing  $\langle S_{\text{Born}}^2 \rangle^{1/2}$  and  $\langle K_{\text{Born}}^2 \rangle^{1/2}$  ( $\sim 5 \times 10^5$ ), even though  $\langle S \rangle$  and  $\langle K \rangle$  are a few orders of magnitude smaller than  $\langle S_{\text{Born}}^2 \rangle^{1/2}$  and  $\langle K_{\text{Born}}^2 \rangle^{1/2}$ . This implies that the average and the variance of  $S$  and  $K$  are equally useful in probing a small scale matter power spectrum.

As for the corrections to the variance, we found that they are less than  $\leq 1\%$  of the Born approximation when the shot noise effect is excluded. We also found that the post-Born corrections become either positive or negative depending on how the matter power spectrum behave at the corresponding Fresnel scale. With these results, we estimated that  $N_{\text{event}} = 1 \times 10^6$  with  $\text{SNR} = 100$  for  $\delta_{S^2, \text{dc}}$  and  $N_{\text{event}} = 1 \times 10^4$  with  $\text{SNR} = 100$  for  $\delta_{K^2, \text{dc}}$  are required for detecting the post-Born effect on the variance. Although the detection of them seems feasible, the difficulty of separating the post-Born signal from the Born signal implies that it is still a challenging measurement requirement. For this reason, considering the post-Born effect on the variance would be unnecessary for the time being unless the shot noise effect is significantly large. Although the shot noise is undoubtedly



the dominant effect at a small scale matter power spectrum, the interpretation of its effect needs to be done carefully. The post-Born corrections could be enhanced by the shot noise and become quite large at a high frequency ( $\langle S \rangle / \langle S_{\text{Born}}^2 \rangle^{1/2}$  and  $\delta_{S^2_{\text{dc}}} / \langle S_{\text{Born}}^2 \rangle$  could become more than 10% at  $f = 10^3$  Hz). We expect that this is caused by a very rare event where the shot noise constituent is almost on the line of sight. In this case, the magnitude of the average and variance would become drastically small by removing these events when taking the ensemble average. However, we have to determine the probability distribution of each event to evaluate the degree of reduction induced by their removal. In addition, we have not included the bispectrum and trispectrum effects in this work, though this could become comparable to the corrections given by accounting for only Gaussianity. These remaining problems need to be addressed in the future.

## Acknowledgements

We would like to thank Ryuichi Takahashi and Adrean Webb for discussions which were quite helpful. This work is supported by the MEXT KAKENHI Grant Number 17H06359 (TS), JP21H05453 (TS), and the JSPS KAKENHI Grant Number JP19K03864 (TS).

## A Geometric optics limit

In [12–16], the post-Born approximation is discussed under geometric optics. Although geometric optics has been widely used in the gravitational lensing, fundamentally more accurate description for the GL of GWs is wave optics. In this sense, wave optics should be able to encompass everything that could be derived in geometric optics.

In geometric optics, we take the large frequency limit ( $\omega \rightarrow \infty$ ) from the outset and start from the geodesic equation which does not contain  $\omega$ . In this appendix, we demonstrate explicitly that the magnification in the high frequency limit under the post-Born approximation in wave optics coincides with the one derived based on geometric optics. In order to calculate the magnification under geometric optics, we need the convergence  $\kappa$  and shear  $\gamma$  up to second order and first order in  $\Phi$ , respectively. According to [12–16], they are given by

$$\kappa^{(1)}(\boldsymbol{\theta}_0, \chi_s) = -2 \int_0^{\chi_s} d\chi \chi^2 W(\chi, \chi_s) \Phi_{ii}(\chi), \quad (\text{A.1})$$

$$\begin{aligned} \kappa^{(2)}(\boldsymbol{\theta}_0, \chi_s) = & -2 \int_0^{\chi_s} d\chi \int_0^\chi d\chi' \chi^2 \chi'^2 W(\chi, \chi_s) W(\chi', \chi) \Phi_{ij}(\chi) \Phi_{ij}(\chi') \\ & -2 \int_0^{\chi_s} d\chi \int_0^\chi d\chi' \chi^3 \chi' W(\chi, \chi_s) W(\chi', \chi) \Phi_{iik}(\chi) \Phi_k(\chi'), \end{aligned} \quad (\text{A.2})$$

$$\gamma_1^{(1)}(\boldsymbol{\theta}_0, \chi_s) = \int_0^{\chi_s} d\chi \chi^2 W(\chi, \chi_s) (\Phi_{11}(\chi) - \Phi_{22}(\chi)), \quad (\text{A.3})$$

$$\gamma_2^{(1)}(\boldsymbol{\theta}_0, \chi_s) = 2 \int_0^{\chi_s} d\chi \chi^2 W(\chi, \chi_s) \Phi_{12}(\chi). \quad (\text{A.4})$$

The gravitational potential is evaluated at the straight line along which the unlensed ray propagates, namely  $\Phi(\chi) = \Phi(\boldsymbol{\theta}_0, \chi)$ . The magnification  $\mu_{\text{geo}}(\boldsymbol{\theta}_0, \chi_s)$  is the inverse of the determinant of the Jacobian matrix  $\mathbf{A}(\boldsymbol{\theta}_0, \chi) = \begin{pmatrix} 1 - \kappa - \gamma_1 & -\gamma_2 - \Omega \\ -\gamma_2 + \Omega & 1 - \kappa + \gamma_1 \end{pmatrix}$  and, up to second order in  $\Phi$ ,  $\mu_{\text{geo}}$  is given by

$$\begin{aligned} \mu_{\text{geo}}(\boldsymbol{\theta}_0, \chi_s) = & 1 + 2\kappa^{(1)} + 2\kappa^{(2)} + 3(\kappa^{(1)})^2 + (\gamma_1^{(1)})^2 + (\gamma_2^{(1)})^2 \\ = & 1 + 2\kappa^{(1)}(\boldsymbol{\theta}_0, \chi_s) + 2(\kappa^{(1)}(\boldsymbol{\theta}_0, \chi_s))^2 \\ & - 4 \int_0^{\chi_s} d\chi \int_0^\chi d\chi' \chi^3 \chi' W(\chi, \chi_s) W(\chi', \chi) \Phi_{iik}(\chi) \Phi_k(\chi') \\ & + 4 \int_0^{\chi_s} d\chi \int_0^\chi d\chi' \chi^2 \chi'^2 W(\chi, \chi_s)^2 \Phi_{ij}(\chi) \Phi_{ij}(\chi'). \end{aligned} \quad (\text{A.5})$$

Up to this order,  $\Omega$  does not appear in the magnification as  $\Omega$  itself is already second order in  $\Phi$ .

We now show the magnification computed in wave optics based on the formulation given in this paper reduces to Eq. (A.5) in the high frequency limit. Prior to that, we

write the approximated solution of the lens equation up to first order in  $\Phi$ .

$$\delta\Theta(\boldsymbol{\theta}_0, \chi) = -2 \int_0^\chi d\chi' W(\chi', \chi) \nabla_\theta \Phi(\boldsymbol{\theta}_0, \chi'). \quad (\text{A.6})$$

In wave optics, the magnification effect is encoded in  $K$  as  $\mu_{\text{wave}}(\boldsymbol{\theta}, \omega) = e^{2K}$ , where  $\boldsymbol{\theta}$  is the position of the source on the source plane  $\boldsymbol{\theta} = \boldsymbol{\theta}_0 + \delta\Theta(\boldsymbol{\theta}_0, \chi_s)$ . Taking  $\omega \rightarrow \infty$  of Eqs. (2.20) and (2.21) yields

$$K^{(1)}(\boldsymbol{\theta}, \chi_s, \omega \rightarrow \infty) = -2 \int_0^{\chi_s} d\chi \chi^2 W(\chi, \chi_s) \Phi_{ii}(\boldsymbol{\theta}, \chi) = \kappa^{(1)}(\boldsymbol{\theta}, \chi_s) \quad (\text{A.7})$$

$$\begin{aligned} K^{(2)}(\boldsymbol{\theta}, \chi_s, \omega \rightarrow \infty) &= \int_0^{\chi_s} \frac{d\chi}{\chi^2} \int_0^\chi d\chi_1 \int_0^\chi d\chi_2 \\ &\quad \times [W(\chi, \chi_s) \nabla_{\theta_{12}}^2 + W(\chi_1, \chi) \nabla_{\theta_1}^2 + W(\chi_2, \chi) \nabla_{\theta_2}^2] \nabla_{\theta_1} \Phi_1 \cdot \nabla_{\theta_2} \Phi_2 \\ &= - \int_0^{\chi_s} d\chi_1 W(\chi_1, \chi_s) \nabla_\theta (\nabla_\theta^2 \Phi(\chi_1)) \cdot (-2) \int_0^{\chi_s} d\chi_2 W(\chi_2, \chi_s) \nabla_\theta \Phi(\chi_2) \\ &\quad - 2 \int_0^{\chi_s} d\chi \int_0^\chi d\chi' \chi^3 \chi' W(\chi, \chi_s) W(\chi', \chi) \Phi_{iik}(\chi) \Phi_k(\chi') \\ &\quad + 2 \int_0^{\chi_s} d\chi \int_0^\chi d\chi' \chi^2 \chi'^2 W(\chi, \chi_s)^2 \Phi_{ij}(\chi) \Phi_{ij}(\chi') \\ &= - \nabla_\theta K^{(1)} \cdot \delta\Theta \\ &\quad - 2 \int_0^{\chi_s} d\chi \int_0^\chi d\chi' \chi^3 \chi' W(\chi, \chi_s) W(\chi', \chi) \Phi_{iik}(\chi) \Phi_k(\chi') \\ &\quad + 2 \int_0^{\chi_s} d\chi \int_0^\chi d\chi' \chi^2 \chi'^2 W(\chi, \chi_s)^2 \Phi_{ij}(\chi) \Phi_{ij}(\chi'). \end{aligned} \quad (\text{A.8})$$

The magnification in wave optics up to second order is then given by

$$\begin{aligned} \mu_{\text{wave}}(\boldsymbol{\theta}, \chi_s, \omega \rightarrow \infty) &= 1 + 2K^{(1)} + 2(K^{(1)})^2 + 2K^{(2)} \\ &= 1 + 2\kappa^{(1)}(\boldsymbol{\theta} - \delta\Theta, \chi_s) + 2(\kappa^{(1)}(\boldsymbol{\theta}_0, \chi_s))^2 \\ &\quad - 4 \int_0^{\chi_s} d\chi \int_0^\chi d\chi' \chi^3 \chi' W(\chi, \chi_s) W(\chi', \chi) \Phi_{iik}(\chi) \Phi_k(\chi') \\ &\quad + 4 \int_0^{\chi_s} d\chi \int_0^\chi d\chi' \chi^2 \chi'^2 W(\chi, \chi_s)^2 \Phi_{ij}(\chi) \Phi_{ij}(\chi') \\ &= \mu_{\text{geo}}(\boldsymbol{\theta}_0, \chi_s). \end{aligned} \quad (\text{A.9})$$

Therefore, the result of geometric optics is indeed derived by taking the high frequency limit of wave optics. It is important to mention again that the lens plane  $\boldsymbol{\theta}_0$  is used in geometric optics whereas, in wave optics, the source plane  $\boldsymbol{\theta}$  is the fundamental variable. This difference manifests itself in the argument of both  $\mu_{\text{geo}}$  and  $\mu_{\text{wave}}$ . We have shown that, at least up to second order in  $\Phi$ , our formulation reduces to the well-known result in geometric optics. This consistency strongly supports the validity of the discussion about the post-Born approximation of the lensing in wave optics.

## B Post-Born variance of $S$ and $K$

The correction of the variance of  $K$  to the Born approximation is described by Eq. (2.36), and similar relation holds for  $S$ . This equation is rewritten by using the matter power spectrum given in Eq. (3.1):

$$\begin{aligned} \delta_{X,\text{dc}} = & 16 \left( \frac{3H_0^2 \Omega_m}{2} \right)^4 \int_0^{\chi_s} \frac{d\chi}{\chi^2} \int_0^\chi \frac{d\chi'}{\chi'^2} \int_0^{\chi'} d\chi_1 \int_0^{\chi'} d\chi_2 \frac{1}{a^2(\chi_1)} \frac{1}{a^2(\chi_2)} \frac{1}{(2\pi)^2} \\ & \times \omega^2 \int_0^\infty dk_1 \int_0^\infty dk_2 P_\delta(k_1, \chi_1) P_\delta(k_2, \chi_2) \left[ \frac{1}{k_1 k_2} \mathcal{F}_{12} - \frac{1}{k_1^2} \mathcal{F}_1 - \frac{1}{k_2^2} \mathcal{F}_2 \right], \end{aligned} \quad (\text{B.1})$$

where

$$\begin{aligned} \mathcal{F}_{12} = & \chi_1^2 \chi_2^2 \int_0^{2\pi} \frac{d\phi}{2\pi} \cos^2 \phi \left\{ F \left( \frac{\chi_1^2 W(\chi_1, \chi_s)}{2\omega} k_1^2 + \frac{\chi_2^2 W(\chi_2, \chi_s)}{2\omega} k_2^2 + \frac{\chi_1 \chi_2 W(\chi, \chi_s)}{\omega} k_1 k_2 \cos \phi \right) \right. \\ & \times F \left( \frac{\chi_1^2 W(\chi_1, \chi_s)}{2\omega} k_1^2 + \frac{\chi_2^2 W(\chi_2, \chi_s)}{2\omega} k_2^2 + \frac{\chi_1 \chi_2 W(\chi', \chi_s)}{\omega} k_1 k_2 \cos \phi \right) \\ & - F \left( \frac{\chi_1^2 W(\chi_1, \chi_s)}{2\omega} k_1^2 \right) F \left( \frac{\chi_1^2 W(\chi_1, \chi_s)}{2\omega} k_1^2 + \frac{\chi_2^2 W(\chi_2, \chi)}{\omega} k_2^2 + \frac{\chi_1 \chi_2 W(\chi', \chi)}{\omega} k_1 k_2 \cos \phi \right) \\ & \left. - F \left( \frac{\chi_2^2 W(\chi_2, \chi_s)}{2\omega} k_2^2 \right) F \left( \frac{\chi_2^2 W(\chi_2, \chi_s)}{2\omega} k_2^2 + \frac{\chi_1^2 W(\chi_1, \chi)}{\omega} k_1^2 + \frac{\chi_1 \chi_2 W(\chi', \chi)}{\omega} k_1 k_2 \cos \phi \right) \right\}, \end{aligned} \quad (\text{B.2})$$

$$\begin{aligned} \mathcal{F}_1 = & \chi_1 \chi_2^3 \int_0^{2\pi} \frac{d\phi}{2\pi} \cos \phi \\ & \times F \left( \frac{\chi_1^2 W(\chi_1, \chi_s)}{2\omega} k_1^2 \right) F \left( \frac{\chi_1^2 W(\chi_1, \chi_s)}{2\omega} k_1^2 + \frac{\chi_2^2 W(\chi_2, \chi)}{\omega} k_2^2 + \frac{\chi_1 \chi_2 W(\chi', \chi)}{\omega} k_1 k_2 \cos \phi \right), \end{aligned} \quad (\text{B.3})$$

$$\begin{aligned} \mathcal{F}_2 = & \chi_2 \chi_1^3 \int_0^{2\pi} \frac{d\phi}{2\pi} \cos \phi \\ & \times F \left( \frac{\chi_2^2 W(\chi_2, \chi_s)}{2\omega} k_2^2 \right) F \left( \frac{\chi_2^2 W(\chi_2, \chi_s)}{2\omega} k_2^2 + \frac{\chi_1^2 W(\chi_1, \chi)}{\omega} k_1^2 + \frac{\chi_1 \chi_2 W(\chi', \chi)}{\omega} k_1 k_2 \cos \phi \right). \end{aligned} \quad (\text{B.4})$$

Here,  $X$  is either  $K^2$  or  $S^2$ .  $F(x)$  is defined as  $F(x) = \sin x$  for the magnification  $K$  and  $F(x) = 1 - \cos x$  for the phase modulation  $S$ . Even though  $\chi_1$  and  $\chi_2$  are symmetrical and can be expressed by either one of two terms, we explicitly write both terms so that the symmetry can be captured easily. The integral with respect to  $\phi$  can be performed

analytically by using the identities regarding Bessel functions:

$$\int_0^{2\pi} \frac{d\phi}{2\pi} \cos \phi \sin(x \cos \phi) = J_1(x), \quad (\text{B.5})$$

$$\int_0^{2\pi} \frac{d\phi}{2\pi} \cos^2 \phi \cos(x \cos \phi) = \frac{1}{2} [J_0(x) - J_2(x)]. \quad (\text{B.6})$$

In addition to this,  $\int_0^{2\pi} \frac{d\phi}{2\pi} \cos \phi \cos(x \cos \phi) = \int_0^{2\pi} \frac{d\phi}{2\pi} \cos^2 \phi \sin(x \cos \phi) = 0$  holds by virtue of the anti-symmetric nature of the integrand.

For the magnification,  $\mathcal{F}_{K,12}, \mathcal{F}_{K,1}, \mathcal{F}_{K,2}$  are given by

$$\begin{aligned} \mathcal{F}_{K,12} = & \frac{\chi_1^2 \chi_2^2}{4} \left\{ \left( 1 - \cos \left( \frac{\chi_1^2 W(\chi_1, \chi)}{\omega} k_1^2 \right) - \cos \left( \frac{\chi_2^2 W(\chi_2, \chi)}{\omega} k_2^2 \right) \right) \right. \\ & + \cos \left( \frac{\chi_1^2 W(\chi_1, \chi_s)}{\omega} k_1^2 + \frac{\chi_2^2 W(\chi_2, \chi)}{\omega} k_2^2 \right) + \cos \left( \frac{\chi_2^2 W(\chi_2, \chi_s)}{\omega} k_2^2 + \frac{\chi_1^2 W(\chi_1, \chi)}{\omega} k_1^2 \right) \\ & \times \left[ J_0 \left( \frac{\chi_1 \chi_2 W(\chi', \chi)}{\omega} k_1 k_2 \right) - J_2 \left( \frac{\chi_1 \chi_2 W(\chi', \chi)}{\omega} k_1 k_2 \right) \right] \\ & - \cos \left( \frac{\chi_1^2 W(\chi_1, \chi_s)}{\omega} k_1^2 + \frac{\chi_2^2 W(\chi_2, \chi_s)}{\omega} k_2^2 \right) \\ & \left. \times \left[ J_0 \left( \frac{\chi_1 \chi_2 W(\chi, \chi_s) + \chi_1 \chi_2 W(\chi', \chi_s)}{\omega} k_1 k_2 \right) - J_2 \left( \frac{\chi_1 \chi_2 W(\chi, \chi_s) + \chi_1 \chi_2 W(\chi', \chi_s)}{\omega} k_1 k_2 \right) \right] \right\}, \end{aligned} \quad (\text{B.7})$$

$$\begin{aligned} \mathcal{F}_{K,1} = & \frac{\chi_1 \chi_2^3}{2} \left\{ \sin \left( \frac{\chi_1^2 W(\chi_1, \chi_s)}{\omega} k_1^2 + \frac{\chi_2^2 W(\chi_2, \chi)}{\omega} k_2^2 \right) - \sin \left( \frac{\chi_2^2 W(\chi_2, \chi)}{\omega} k_2^2 \right) \right\} \\ & \times J_1 \left( \frac{\chi_1 \chi_2 W(\chi', \chi)}{\omega} k_1 k_2 \right), \end{aligned} \quad (\text{B.8})$$

$$\begin{aligned} \mathcal{F}_{K,2} = & \frac{\chi_2 \chi_1^3}{2} \left\{ \sin \left( \frac{\chi_2^2 W(\chi_2, \chi_s)}{\omega} k_2^2 + \frac{\chi_1^2 W(\chi_1, \chi)}{\omega} k_1^2 \right) - \sin \left( \frac{\chi_1^2 W(\chi_1, \chi)}{\omega} k_1^2 \right) \right\} \\ & \times J_1 \left( \frac{\chi_1 \chi_2 W(\chi', \chi)}{\omega} k_1 k_2 \right). \end{aligned} \quad (\text{B.9})$$

In exactly the same way, the similar equations are derived for the phase modulation:

$$\begin{aligned}
\mathcal{F}_{S,12} = & \chi_1^2 \chi_2^2 \left\{ -\frac{1}{2} + \frac{1}{2} \cos \left( \frac{\chi_1^2 W(\chi_1, \chi_s)}{2\omega} k_1^2 \right) + \frac{1}{2} \cos \left( \frac{\chi_2^2 W(\chi_2, \chi_s)}{2\omega} k_2^2 \right) \right. \\
& - \frac{1}{2} \cos \left( \frac{\chi_1^2 W(\chi_1, \chi_s)}{2\omega} k_1^2 + \frac{\chi_2^2 W(\chi_2, \chi_s)}{2\omega} k_2^2 \right) \\
& \times \left[ J_0 \left( \frac{\chi_1 \chi_2 W(\chi, \chi_s)}{\omega} k_1 k_2 \right) + J_0 \left( \frac{\chi_1 \chi_2 W(\chi', \chi_s)}{\omega} k_1 k_2 \right) \right. \\
& \left. - J_2 \left( \frac{\chi_1 \chi_2 W(\chi, \chi_s)}{\omega} k_1 k_2 \right) - J_2 \left( \frac{\chi_1 \chi_2 W(\chi', \chi_s)}{\omega} k_1 k_2 \right) \right] \\
& + \frac{1}{4} \cos \left( \frac{\chi_1^2 W(\chi_1, \chi_s)}{\omega} k_1^2 + \frac{\chi_2^2 W(\chi_2, \chi_s)}{\omega} k_2^2 \right) \\
& \times \left[ J_0 \left( \frac{\chi_1 \chi_2 W(\chi, \chi_s) + \chi_1 \chi_2 W(\chi', \chi_s)}{\omega} k_1 k_2 \right) - J_2 \left( \frac{\chi_1 \chi_2 W(\chi, \chi_s) + \chi_1 \chi_2 W(\chi', \chi_s)}{\omega} k_1 k_2 \right) \right] \\
& + \left( \frac{1}{4} + \sin^2 \left( \frac{\chi_1^2 W(\chi_1, \chi_s)}{4\omega} k_1^2 \right) \cos \left( \frac{\chi_1^2 W(\chi_1, \chi_s)}{2\omega} k_1^2 + \frac{\chi_2^2 W(\chi_2, \chi)}{\omega} k_2^2 \right) \right. \\
& \left. + \sin^2 \left( \frac{\chi_2^2 W(\chi_2, \chi_s)}{4\omega} k_2^2 \right) \cos \left( \frac{\chi_2^2 W(\chi_2, \chi_s)}{2\omega} k_2^2 + \frac{\chi_1^2 W(\chi_1, \chi)}{\omega} k_1^2 \right) \right) \\
& \times \left[ J_0 \left( \frac{\chi_1 \chi_2 W(\chi', \chi)}{\omega} k_1 k_2 \right) - J_2 \left( \frac{\chi_1 \chi_2 W(\chi', \chi)}{\omega} k_1 k_2 \right) \right] \left. \right\}, \tag{B.10}
\end{aligned}$$

$$\begin{aligned}
\mathcal{F}_{S,1} = & 2\chi_1 \chi_2^3 \sin^2 \left( \frac{\chi_1^2 W(\chi_1, \chi_s)}{4\omega} k_1^2 \right) \sin \left( \frac{\chi_1^2 W(\chi_1, \chi_s)}{2\omega} k_1^2 + \frac{\chi_2^2 W(\chi_2, \chi)}{\omega} k_2^2 \right) \\
& \times J_1 \left( \frac{\chi_1 \chi_2 W(\chi', \chi)}{\omega} k_1 k_2 \right), \tag{B.11}
\end{aligned}$$

$$\begin{aligned}
\mathcal{F}_{S,2} = & 2\chi_2 \chi_1^3 \sin^2 \left( \frac{\chi_2^2 W(\chi_2, \chi_s)}{4\omega} k_2^2 \right) \sin \left( \frac{\chi_2^2 W(\chi_2, \chi_s)}{2\omega} k_2^2 + \frac{\chi_1^2 W(\chi_1, \chi)}{\omega} k_1^2 \right) \\
& \times J_1 \left( \frac{\chi_1 \chi_2 W(\chi', \chi)}{\omega} k_1 k_2 \right). \tag{B.12}
\end{aligned}$$

## C High frequency behavior of $\delta_{S^2, \text{dc}}$

In this appendix, we would like to approximately derive the high frequency behavior of  $\delta_{S^2, \text{dc}}$  in order to avoid the difficulty of numerical computation associated with the cancellation of significant digits. When the frequency of GWs is high,  $\delta_{S^2, \text{dc}}$  is mainly affected by the large  $k$  region of the matter power spectrum. As shown in Fig. 1,  $P_\delta$  follows the simple power-law at large  $k$ , namely,

$$P_\delta(k, \chi) = B(\chi) k^{-b} \quad (k_L \leq k). \tag{C.1}$$

$b$  only fluctuates around a certain value and, in our model, we take  $b = 2.87$  at  $z = 0$ . Therefore, it is not constructive to consider unusually big or small  $b$ . Keeping this in mind, we only consider the case that is relevant to our discussion.

We usually deal with the GW sources whose distance from the earth is roughly given by  $1/H_0$ , so the corresponding Fresnel scale is  $1/\sqrt{\omega H_0}$ . The high frequency behavior in this context is then interpreted as the satisfaction of the condition  $k_L \ll \sqrt{H_0 \omega}$ . Defining  $\int \cdots \int \equiv 16 \left( \frac{3H_0^2 \Omega_m}{2} \right)^4 \int_0^{\chi_s} \frac{d\chi}{\chi^2} \int_0^\chi \frac{d\chi'}{\chi'^2} \int_0^{\chi'} d\chi_1 \int_0^{\chi'} d\chi_2 \frac{1}{a^2(\chi_1)} \frac{1}{a^2(\chi_2)} \frac{1}{(2\pi)^2}$ , the post-Born approximation of the variance of  $S$  is given by

$$\delta_{S^2, \text{dc}} = \int \cdots \int \omega^2 \int_0^\infty dk_1 \int_0^\infty dk_2 P_\delta(k_1, \chi_1) P_\delta(k_2, \chi_2) \left[ \frac{1}{k_1 k_2} \mathcal{F}_{S,12} - \frac{1}{k_1^2} \mathcal{F}_{S,1} - \frac{1}{k_2^2} \mathcal{F}_{S,2} \right], \quad (\text{C.2})$$

The definition of  $\mathcal{F}_{S,12}$ ,  $\mathcal{F}_{S,1}$ ,  $\mathcal{F}_{S,2}$  is the same as the ones in Appendix B. Change of variable  $k_1 = \sqrt{\omega} \xi_1$ ,  $k_2 = \sqrt{\omega} \xi_2$  and separating the integral area at  $k_L$  yield

$$\begin{aligned} \delta_{S^2, \text{dc}} = & \int \cdots \int \omega^2 \int_0^{\frac{k_L}{\sqrt{\omega}}} d\xi_1 \int_0^{\frac{k_L}{\sqrt{\omega}}} d\xi_2 P_\delta(\sqrt{\omega} \xi_1, \chi_1) P_\delta(\sqrt{\omega} \xi_2, \chi_2) \left[ \frac{1}{\xi_1 \xi_2} \mathcal{F}_{12} - \frac{1}{\xi_1^2} \mathcal{F}_1 - \frac{1}{\xi_2^2} \mathcal{F}_2 \right] \\ & + \int \cdots \int \omega^{2-\frac{b}{2}} B(\chi_2) \int_0^{\frac{k_L}{\sqrt{\omega}}} d\xi_1 \int_{\frac{k_L}{\sqrt{\omega}}}^\infty d\xi_2 P_\delta(\sqrt{\omega} \xi_1, \chi_1) \xi_2^{-b} \left[ \frac{1}{\xi_1 \xi_2} \mathcal{F}_{12} - \frac{1}{\xi_1^2} \mathcal{F}_1 - \frac{1}{\xi_2^2} \mathcal{F}_2 \right] \\ & + \int \cdots \int \omega^{2-\frac{b}{2}} B(\chi_1) \int_{\frac{k_L}{\sqrt{\omega}}}^\infty d\xi_1 \int_0^{\frac{k_L}{\sqrt{\omega}}} d\xi_2 P_\delta(\sqrt{\omega} \xi_2, \chi_2) \xi_1^{-b} \left[ \frac{1}{\xi_1 \xi_2} \mathcal{F}_{12} - \frac{1}{\xi_1^2} \mathcal{F}_1 - \frac{1}{\xi_2^2} \mathcal{F}_2 \right] \\ & + \int \cdots \int \omega^{2-b} B(\chi_1) B(\chi_2) \int_{\frac{k_L}{\sqrt{\omega}}}^\infty d\xi_1 \int_{\frac{k_L}{\sqrt{\omega}}}^\infty d\xi_2 \xi_2^{-b} \xi_1^{-b} \left[ \frac{1}{\xi_1 \xi_2} \mathcal{F}_{12} - \frac{1}{\xi_1^2} \mathcal{F}_1 - \frac{1}{\xi_2^2} \mathcal{F}_2 \right]. \end{aligned} \quad (\text{C.3})$$

Since these four terms contribute to  $\delta_{S^2, \text{dc}}$  in a different way, we will compute the contribution from each term separately. To begin with, we consider the first term. In the high frequency limit, the integral range  $\int_0^{\frac{k_L}{\sqrt{\omega}}}$  is restricted in a very small area so the contribution from the first term in Eq. (C.3) comes from the region where  $\xi_1, \xi_2 \ll 1$  holds. Since  $\xi_1$  and  $\xi_2$  are both order  $1/\sqrt{\omega}$  in this integral range, the expansion of  $\mathcal{F}$  in  $1/\sqrt{\omega}$  up to leading order yields  $\mathcal{F} = \mathcal{O}(1/\omega^4)$ . Considering that  $\omega^2$  is multiplied in the expression, we can conclude that the first term is proportional to  $\omega^{-2}$ .

The second and third terms in Eq. (C.3) are symmetrical with respect to the subscript 1,2, so they have the same contribution. In the second term,  $\xi_1$  is still restricted in the area where  $\xi_1 \ll 1$  whereas  $\xi_2$  is no longer small. In this case, we can expand  $\mathcal{F}$  only in



terms of  $\xi_1$  and keep  $\xi_2$  term untouched then we have

$$\begin{aligned} \mathcal{F} = & \xi_1 \left[ \xi_2 \left( \cos \left( \frac{\chi_2^2 W(\chi_2, \chi_s)}{2} \xi_2^2 \right) - \cos^2 \left( \frac{\chi_2^2 W(\chi_2, \chi_s)}{2} \xi_2^2 \right) \right) C \right. \\ & \left. + \left( \frac{\sin \left( \frac{\chi_2^2 W(\chi_2, \chi_s)}{2} \xi_2^2 \right)}{2\xi_2} - \frac{\sin(\chi_2^2 W(\chi_2, \chi_s) \xi_2^2)}{4\xi_2} \right) D_1 + C \xi_2 \sin^2 \left( \frac{\chi_2^2 W(\chi_2, \chi_s)}{2} \xi_2^2 \right) \right] + \mathcal{O}(\xi_1^3). \end{aligned} \quad (\text{C.4})$$

where  $C, D_1$  are

$$C = \frac{3}{8} \chi_1^4 \chi_2^4 W(\chi, \chi_s) W(\chi', \chi_s), \quad (\text{C.5})$$

$$D_1 = \chi_1^6 \chi_2^2 \{-W(\chi', \chi) + W(\chi, \chi_s)\}. \quad (\text{C.6})$$

Combining these notations, the second term is calculated as

$$\begin{aligned} (\text{2nd}) &= \int \cdots \int \omega^{2-\frac{b}{2}} B(\chi_2) \int_0^{\frac{k_L}{\sqrt{\omega}}} d\xi_1 P_\delta(\sqrt{\omega} \xi_1, \chi_1) \int_{\frac{k_L}{\sqrt{\omega}}}^\infty d\xi_2 \xi_2^{-b} \left[ \frac{1}{\xi_1 \xi_2} \mathcal{F}_{12} - \frac{1}{\xi_1^2} \mathcal{F}_1 - \frac{1}{\xi_2^2} \mathcal{F}_2 \right] \\ &= \frac{1}{\omega^{\frac{b}{2}-1}} \int \cdots \int B(\chi_2) \int_0^\infty dk_1 k_1 P_\delta(k_1, \chi_1) \int_0^\infty d\xi_2 \frac{1}{\xi_2^b} [(\cdots)C + (\cdots)D_1 + (\cdots)C] \\ &= \frac{1}{\omega^{\frac{b}{2}-1}} \int \cdots \int B(\chi_2) \int_0^\infty dk_1 k_1 P_\delta(k_1, \chi_1) \left( \frac{\chi_2^2 W(\chi_2, \chi_s)}{2} \right)^{\frac{b-2}{2}} \left[ CI_c + \frac{2}{\chi_2^2 W(\chi_2, \chi_s)} D_1 I_d + CI_e \right]. \end{aligned} \quad (\text{C.7})$$

From the first line to the second, we used Eq. (C.4), and took the integral range from zero to infinity. We can safely perform this approximation due to the fact that the integral converges. Here,  $I_c, I_d, I_e$  are just numbers defined as

$$I_c = \int_0^\infty dx \frac{\cos x^2 - \cos^2 x^2}{x^{b-1}}, \quad (\text{C.8})$$

$$I_d = \int_0^\infty dx \frac{2 \sin x^2 - \sin 2x^2}{4x^{b+1}}, \quad (\text{C.9})$$

$$I_e = \int_0^\infty dx \frac{\sin^2 x^2}{x^{b-1}}. \quad (\text{C.10})$$

The fourth term in Eq. (C.3) is calculated in a similar way,

$$\begin{aligned} (\text{4th}) &= \frac{1}{\omega^{\frac{b}{2}-1}} \int \cdots \int B(\chi_1) B(\chi_2) \frac{k_L^{-b+2}}{b-2} \\ &\quad \times \left\{ \left( \frac{\chi_2^2 W(\chi_2, \chi_s)}{2} \right)^{\frac{b-2}{2}} \left[ CI_c + \frac{2}{\chi_2^2 W(\chi_2, \chi_s)} D_1 I_d + CI_e \right] + (1 \iff 2) \right\}. \end{aligned} \quad (\text{C.11})$$

Note that the fourth term is essentially determined by  $k_L$ , which is the arbitrary scale. However, the second term and the third term are determined by the scale at which  $P_\delta$  changes from an increasing function to a decreasing function due to the dependence on  $\int_0^\infty dk_1 k_1 P_\delta(k_1)$ . Since we can take  $k_L$  to be sufficiently larger than this scale, it is justified to ignore the contribution from the fourth term. Finally, we obtain the following asymptotic behavior of  $\delta_{S^2,dc}$  for large  $\omega$ :

$$\delta_{S^2,dc} = 2 \times \frac{1}{\omega^{\frac{b}{2}-1}} \times 16 \left( \frac{3H_0^2 \Omega_m}{2} \right)^4 \int_0^{\chi_s} \frac{d\chi}{\chi^2} \int_0^\chi \frac{d\chi'}{\chi'^2} \int_0^{\chi'} d\chi_1 \int_0^{\chi'} d\chi_2 \frac{1}{a^2(\chi_1)} \frac{1}{a^2(\chi_2)} \frac{1}{(2\pi)^2} \\ \times B(\chi_2) \int_0^\infty dk_1 k_1 P_\delta(k_1, \chi_1) \left[ CI_c + \frac{2}{\chi_2^2 W(\chi_2, \chi_s)} D_1 I_d + CI_e \right] \left( \frac{\chi_2^2 W(\chi_2, \chi_s)}{2} \right)^{\frac{b-2}{2}} \quad (\text{C.12})$$

## References

- [1] M. Bartelmann, *Gravitational Lensing*, *Class. Quant. Grav.* **27** (2010) 233001, [[arXiv:1010.3829](#)].
- [2] R. Mandelbaum, *Weak lensing for precision cosmology*, *Ann. Rev. Astron. Astrophys.* **56** (2018) 393–433, [[arXiv:1710.03235](#)].
- [3] M. Oguri, *Strong gravitational lensing of explosive transients*, *Rept. Prog. Phys.* **82** (2019), no. 12 126901, [[arXiv:1907.06830](#)].
- [4] C. Misner, K. Thorne, and J. Wheeler, *Gravitation*. W. H. Freeman and Company, 1973.
- [5] H. C. Ohanian, *On the focusing of gravitational radiation*, *Int. J. Theor. Phys.* **9** (1974) 425–437.
- [6] R. Takahashi and T. Nakamura, *Wave effects in gravitational lensing of gravitational waves from chirping binaries*, *Astrophys. J.* **595** (2003) 1039–1051, [[astro-ph/0305055](#)].
- [7] T. T. Nakamura, *Gravitational lensing of gravitational waves from inspiraling binaries by a point mass lens*, *Phys. Rev. Lett.* **80** (1998) 1138–1141.
- [8] T. T. Nakamura and S. Deguchi, *Wave Optics in Gravitational Lensing*, *Prog. Theor. Phys. Suppl.* **133** (1999) 137–153.
- [9] R. Takahashi, *Amplitude and phase fluctuations for gravitational waves propagating through inhomogeneous mass distribution in the universe*, *Astrophys. J.* **644** (2006) 80–85, [[astro-ph/0511517](#)].

- [10] M. Oguri and R. Takahashi, *Probing Dark Low-mass Halos and Primordial Black Holes with Frequency-dependent Gravitational Lensing Dispersions of Gravitational Waves*, *Astrophys. J.* **901** (2020), no. 1 58, [[arXiv:2007.01936](#)].
- [11] M. Oguri and R. Takahashi, *Amplitude and phase fluctuations of gravitational waves magnified by strong gravitational lensing*, [arXiv:2204.00814](#).
- [12] C. Shapiro and A. Cooray, *The born and lens-lens corrections to weak gravitational lensing angular power spectra*, *JCAP* **03** (2006) 007, [[astro-ph/0601226](#)].
- [13] S. Hilbert, J. Hartlap, S. D. M. White, and P. Schneider, *Ray-tracing through the Millennium Simulation: Born corrections and lens-lens coupling in cosmic shear and galaxy-galaxy lensing*, *Astron. Astrophys.* **499** (2009) 31, [[arXiv:0809.5035](#)].
- [14] E. Krause and C. M. Hirata, *Weak lensing power spectra for precision cosmology: Multiple-deflection, reduced shear and lensing bias corrections*, *Astron. Astrophys.* **523** (2010) A28, [[arXiv:0910.3786](#)].
- [15] G. Pratten and A. Lewis, *Impact of post-Born lensing on the CMB*, *JCAP* **08** (2016) 047, [[arXiv:1605.05662](#)].
- [16] A. Petri, Z. Haiman, and M. May, *Validity of the Born approximation for beyond Gaussian weak lensing observables*, *Phys. Rev. D* **95** (2017), no. 12 123503, [[arXiv:1612.00852](#)].
- [17] P. Schneider, E. Jurgen, and F. Emilio, *Gravitational Lenses*. Springer-Verlag, 1992.
- [18] S. Dodelson, *Modern Cosmology*. Academic Press, 2003.
- [19] M. Inamori and T. Suyama, *Universal Relation between the Variances of Distortions of Gravitational Waves owing to Gravitational Lensing*, *Astrophys. J. Lett.* **918** (2021), no. 2 L30, [[arXiv:2107.02443](#)].
- [20] M. Fukugita, C. J. Hogan, and P. J. E. Peebles, *The Cosmic baryon budget*, *Astrophys. J.* **503** (1998) 518, [[astro-ph/9712020](#)].
- [21] P. Villanueva-Domingo, O. Mena, and S. Palomares-Ruiz, *A brief review on primordial black holes as dark matter*, *Front. Astron. Space Sci.* **8** (2021) 87, [[arXiv:2103.12087](#)].
- [22] L. Lindblom, B. J. Owen, and D. A. Brown, *Model waveform accuracy standards for gravitational wave data analysis*, *Phys. Rev. D* **78** (Dec, 2008) 124020, [[arXiv:0809.3844](#)].
- [23] B. P. Abbott, *Exploring the sensitivity of next generation gravitational wave detectors*, *Classical and Quantum Gravity* **34** (jan, 2017) 044001.